Cell Reports
Medicine

Article

Impact of SARS-CoV-2 variants on the total CD4$^+$ and CD8$^+$ T cell reactivity in infected or vaccinated individuals

Graphical abstract

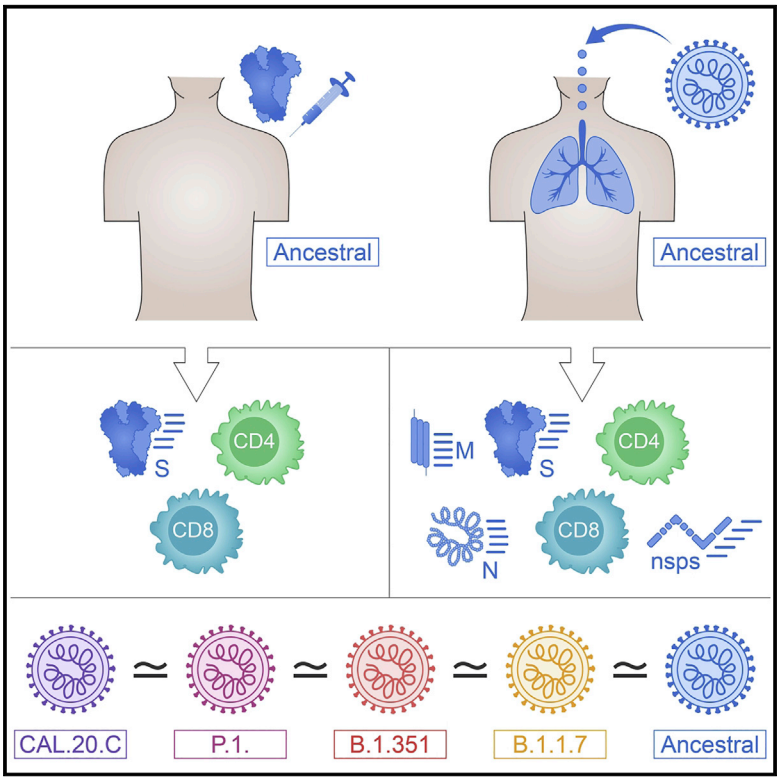

Highlights

- T cells of exposed donors or vaccinees effectively recognize SARS-CoV-2 variants
- Effective recognition in AIM and FluoroSPOT assays, for spike and other proteins
- 93% and 97% of CD4 and CD8 epitopes are 100% conserved across variants

Authors

Alison Tarke, John Sidney, Nils Methot, ..., Shane Crotty, Alba Grifoni, Alessandro Sette

Correspondence

agrifoni@lji.org (A.G.),
alex@lji.org (A.S.)

In brief

Tarke et al. show that SARS-CoV-2-specific memory CD4 and CD8 T cells exposed to the ancestral strain by infection or vaccination effectively recognize the variants B.1.1.7, B.1.351, P.1, and CAL.20C. The majority of T cell epitopes are unaffected by mutations in these variant strains.

Tarke et al., 2021, Cell Reports Medicine 2, 100355
July 20, 2021
https://doi.org/10.1016/j.xcrm.2021.100355

CellPress

Cell Reports Medicine

CellPress
OPEN ACCESS

Article

Impact of SARS-CoV-2 variants on the total CD4+ and CD8+ T cell reactivity in infected or vaccinated individuals

Alison Tarke,[1,2] John Sidney,[1] Nils Methot,[1] Esther Dawen Yu,[1] Yun Zhang,[4] Jennifer M. Dan,[1,3] Benjamin Goodwin,[1] Paul Rubiro,[1] Aaron Sutherland,[1] Eric Wang,[1] April Frazier,[1] Sydney I. Ramirez,[1,3] Stephen A. Rawlings,[3] Davey M. Smith,[3] Ricardo da Silva Antunes,[1] Bjoern Peters,[1,3] Richard H. Scheuermann,[1,4,5] Daniela Weiskopf,[1] Shane Crotty,[1,3] Alba Grifoni,[1,6,*] and Alessandro Sette[1,3,6,7,*]

[1]Center for Infectious Disease and Vaccine Research, La Jolla Institute for Immunology (LJI), La Jolla, CA 92037, USA
[2]Department of Internal Medicine and Center of Excellence for Biomedical Research (CEBR), University of Genoa, Genoa 16132, Italy
[3]Department of Medicine, Division of Infectious Diseases and Global Public Health, University of California, San Diego (UCSD), La Jolla, CA 92037, USA
[4]J. Craig Venter Institute, La Jolla, CA 92037, USA
[5]Department of Pathology, University of California, San Diego, San Diego, CA 92093, USA
[6]These authors contributed equally
[7]Lead contact
*Correspondence: agrifoni@lji.org (A.G.), alex@lji.org (A.S.)
https://doi.org/10.1016/j.xcrm.2021.100355

SUMMARY

The emergence of SARS-CoV-2 variants with evidence of antibody escape highlight the importance of addressing whether the total CD4+ and CD8+ T cell recognition is also affected. Here, we compare SARS-CoV-2-specific CD4+ and CD8+ T cells against the B.1.1.7, B.1.351, P.1, and CAL.20C lineages in COVID-19 convalescents and in recipients of the Moderna (mRNA-1273) or Pfizer/BioNTech (BNT162b2) COVID-19 vaccines. The total reactivity against SARS-CoV-2 variants is similar in terms of magnitude and frequency of response, with decreases in the 10%–22% range observed in some assay/VOC combinations. A total of 7% and 3% of previously identified CD4+ and CD8+ T cell epitopes, respectively, are affected by mutations in the various VOCs. Thus, the SARS-CoV-2 variants analyzed here do not significantly disrupt the total SARS-CoV-2 T cell reactivity; however, the decreases observed highlight the importance for active monitoring of T cell reactivity in the context of SARS-CoV-2 evolution.

INTRODUCTION

The emergence of several severe acute respiratory syndrome-coronavirus-2 (SARS-CoV-2) variants of concern (VOC) with multiple amino acid replacements has implications for the future control of the coronavirus disease 2019 (COVID-19) pandemic.[1–4] VOCs include the United Kingdom (UK) variant 501Y.V1 lineage B.1.1.7,[3] the South Africa (SA) variant 501Y.V2 lineage B.1.351,[4] the BR (Brazilian) variant 501Y.V3 lineage P.1,[5,6] and the California (CA) variant CAL.20C lineages B.1.427–429.[7,8] The B.1.1.7 variant is associated with increased transmissibility,[9,10] and similar epidemiological observations have been reported for the SA and BR variants.[4,5]

The mutations of greatest concern are present in the viral spike (S) protein and include notable mutations in the receptor-binding domain (RBD), the N-terminal domain (NTD), and the furin cleavage site region. Several of the RBD mutations directly affect angiotensin-converting enzyme 2 (ACE2) receptor-binding affinity, which may affect infectivity, viral load, or transmissibility.[11–14] Multiple mutations were also noted in regions bound by neutralizing antibodies, so it is crucial to address the extent to which mutations associated with the variants may affect immunity induced by either SARS-CoV-2 infection or vaccination.

Numerous reports address the effect of variant spike (S) mutations on antibody binding and function.[11,14–23] In general, the impact of B.1.1.7 mutations on neutralizing antibody titers is moderate.[15–18,20,24] In contrast, mutations in B.1.351 and P.1 variants are associated with the more pronounced loss of neutralizing capacity.[15,16,22,23,25] Concerning vaccination responses, the AstraZeneca ChAdOx1 vaccine has been associated with a partial loss of neutralizing antibody activity against B.1.1.7[15] and a large loss of neutralizing activity against B.1.351.[26] ChAdOx1 maintains efficacy against B.1.1.7[24,27] but has a major loss in efficacy against mild COVID-19 with the B.1.351 variant.[26] Current epidemiological evidence is that the BNT162b2 Pfizer/BioNTech COVID-19 vaccine retains its efficacy against B.1.1.7 in the UK[24] and in reports from Israel.[28,29] The Novavax COVID-19 vaccine (NVX-CoV2373) has differential protective immunity against the parental strain, B.1.1.7, and B.1.351 in clinical trials (96%, 86%, and 60%, respectively),[30] whereas the Janssen Ad26.COV2.S 1-dose COVID-19 vaccine has relatively similar protection for moderate COVID-19 against

both the ancestral strain and B.1.351 (72% and 64%, respectively).[31,32]

Several lines of evidence suggest that CD4$^+$ and CD8$^+$ T cell responses play important roles in the resolution of SARS-CoV-2 infection and COVID-19,[33] including modulating disease severity in humans[34,35] and reducing viral loads in non-human primates.[36] Furthermore, individuals with agammaglobulinemia or pharmaceutical depletion of B cells generally experience an uncomplicated COVID-19 disease course.[33,37,38] Robust CD4$^+$ and CD8$^+$ T cell memory is induced after COVID-19,[22,39–41] and multiple COVID-19 vaccines elicit CD4$^+$ and CD8$^+$ T cell responses.[26,42–45] It is therefore key to address the potential impact of mutations associated with SARS-CoV-2 variants on T cell reactivity; however, few data are available on this topic.[46]

Here, we take a combined experimental and bioinformatics approach to address T cell reactivity to SARS-CoV-2 VOCs. We directly assess T cell responses from individuals recovered from COVID-19 and T cell responses from recent Moderna mRNA-1273 or Pfizer/BioNTech BNT162b2 vaccinees for their capacity to recognize peptides derived from the ancestral reference sequence and the B.1.1.7, B1.351, P.1, and CAL.20C variants. As a complementary approach, bioinformatics analyses were used to predict the impact of mutations in the VOCs with sets of previously reported CD4$^+$ and CD8$^+$ T cell epitopes derived from the ancestral reference sequence.

RESULTS

Sequence analysis and peptide pool generation

As a first step, we mapped the specific mutations (amino acid replacements and deletions) of the main current VOCs, including B.1.1.7, B1.351, P.1, and CAL.20C, as compared to the SARS-CoV-2 Wuhan ancestral sequence (NCBI: NC_045512.2) (Table S1). Then, we synthesized the corresponding peptides associated with the different variants and generated new peptide pools (megapools [MPs]) spanning the full genome sequences of the ancestral Wuhan strain and the respective B.1.1.7, B1.351, P.1, and CAL.20C variants (Table S2). As described below, the resulting peptide pools were assessed for their capacity to be recognized by memory T cell responses derived from natural infection in convalescents and vaccinees, and responses to the variant and ancestral genome antigen-specific pools were compared.

Cohorts of COVID-19 convalescent, vaccinees, and unexposed controls

We selected three donor cohorts to investigate T cell reactivity against VOCs. Our convalescent donors were adults ranging from 20 to 67 years of age (median 38); 43% were male and 57% were female (Table 1). SARS-CoV-2 infection in these donors was determined by PCR-based testing during the acute phase of their infection, if available (46% of the cases), and/or seropositivity determined by plasma SARS-CoV-2 S protein RBD immunoglobulin G (IgG) ELISA (Figure S1A). From these donors, peripheral blood mononuclear cell (PBMC) samples were collected between May and October 2020, a period when none of the VOCs analyzed were prevalent in the San Diego, California, area, where the donations from convalescent donors were obtained. The convalescent donor samples reflect the local ethnic demographics (81% non-Hispanic white). The peak of COVID-19 severity was representative of the distribution observed in the general population, with a prevalence of mild cases (86% of the cohort analyzed).

From the vaccinated donors, we collected PBMCs after recent vaccination with the Moderna mRNA-1273 or the Pfizer/BioNTech BNT162b2 vaccines, ~14 days following second dose administration (Table 1). These donors ranged in age from 23 to 67 years (median 47); 31% were male and 69% were female. All of the vaccinees had RBD IgG titers indicative of vaccination (Figure S1A).

PBMCs from unexposed donors were collected between May 2014 and March 2018 or in the March–May 2020 period, and were seronegative for RBD IgG. The unexposed donors ranged from 21 to 82 years old (median 34); 35% were male and 56% were female, while 9% were unknown (Table 1).

CD4$^+$ and CD8$^+$ T cell reactivity against ancestral S

We previously described the use of activation-induced marker (AIM) assays to measure CD4$^+$ and CD8$^+$ T cell responses to pools of overlapping peptides spanning SARS-CoV-2 antigens.[34,39,47,48] Here, we used the same AIM techniques using OX40$^+$CD137$^+$ and CD69$^+$CD137$^+$ markers for CD4$^+$ and CD8$^+$ T cell reactivity, respectively.

We compared the CD4$^+$ and CD8$^+$ T cell reactivity of the three cohorts against SARS-CoV-2 S by AIM and FluoroSPOT assays. The T cell responses to the ancestral S MP were significantly higher than the DMSO controls in unexposed ($p < 0.0001$ for CD4, $p = 0.0063$ for CD8, and $p = 0.0036$ for spot-forming cells [SFCs]/10^6 PBMCs by the Wilcoxon test), convalescent ($p < 0.0001$ for CD4, $p < 0.0001$ for CD8, and $p = 0.0008$ for SFC/10^6 PBMCs by the Wilcoxon test), and vaccinated donors ($p < 0.0001$ for CD4, $p < 0.0001$ for CD8, and $p < 0.0001$ for SFC/10^6 PBMCs by the Wilcoxon test) (Figures S1B–S1D).

When the AIM responses in the different donor cohorts were compared, we found significantly higher reactivity in COVID-19 convalescents compared to unexposed individuals (CD4: $p < 0.0001$; CD8: $p < 0.0001$ by the Mann-Whitney test) (Figures S1E and S1F), with 93% and 39% of donors positive (responses above the threshold of positivity as described in Method details) for CD4$^+$ and CD8$^+$ T cell responses, respectively. These rates of positivity are similar to what was observed in a previous study that analyzed responses to peptides spanning the whole SARS-CoV-2 proteome over a similar range of post-symptom onset (PSO) days,[39] in which 93% and 50% positivity rates were observed for CD4$^+$ and CD8$^+$ T cells, respectively. Likewise, the responses observed in the S MP in vaccinated donors were significantly higher than in unexposed donors (CD4: $p < 0.0001$; CD8: $p < 0.0001$ by Mann-Whitney test), with 100% and 48% of donors positive for CD4 and CD8 responses, respectively (Figures S1E and S1F).

With an interferon-γ (IFN-γ) FluoroSPOT assay, IFN-γ T cell responses were detected in 17%, 50%, and 76% of unexposed, convalescent, and vaccinated donors, respectively (unexposed versus convalescent: $p = 0.019$; unexposed versus vaccinees: $p < 0.0001$ by the Mann-Whitney test) (Figure S1G). These donor T cell responses provided the benchmarks for subsequent assessment of the impact of VOC mutations.

Table 1. Characteristics of donor cohorts

	COVID-19 (n = 28)	Vaccinees (n = 29)	Unexposed (n = 23)
Age, y	20–67 (median = 38, IQR = 32)	23–67 (median = 47, IQR = 36)	21–82 (median = 34, IQR = 24)
Gender, %			
Male	43 (12/28)	31 (9/29)	35 (8/23)
Female	57 (16/28)	69 (20/29)	56 (13/23)
Unknown	0 (0/28)	0 (0/29)	9 (2/23)
Sample collection date	May–October 2020	January–March 2021	May 2014–March 2018 (13/23) March–May 2020 (10/23)
SARS-CoV-2 PCR, %	positive 92 (12/13) not tested 54 (15/28)	N/A	N/A
S RBD IgG$^+$ (%)	96 (27/28)	100 (29/29)	0 (10/10, collected in 2020)
Peak disease severity, %[a]			
Mild	86 (24/28)	N/A	N/A
Moderate	14 (4/28)		
Severe	0 (0/28)		
Critical	0 (0/28)		
Race-ethnicity, %			
White—not Hispanic or Latino	81 (23/28)	52 (15/29)	43 (10/23)
Hispanic or Latino	4 (1/28)	10 (3/29)	9 (2/23)
Asian	7 (2/28)	38 (11/29)	26 (6/23)
American Indian/Alaska Native	0 (0/28)	0 (0/29)	0 (0/23)
Black or African American	0 (0/28)	0 (0/29)	9 (2/23)
>1 race	4 (1/28)	0 (0/29)	4 (1/23)
Not reported	4 (1/28)	0 (0/29)	9 (2/23)
Days at collection	38–163 (28/28) (median = 78, IQR = 50)[b]	13–30 (14/29) Pfizer 12–16 (15/29) Moderna (median = 14, IQR = 14)[c]	N/A

[a]According to World Health Organization criteria.
[b]Post-symptom onset.
[c]2nd dose of vaccine.

CD4$^+$ and CD8$^+$ T cell reactivity against VOC S protein

We measured the CD4$^+$ and CD8$^+$ T cell responses to S MPs derived from the ancestral strain and corresponding MPs representing the B.1.1.7, B1.351, P.1, and CAL.20C variants. As shown in Figures 1A–1C, good CD4$^+$ and CD8$^+$ T cell reactivity was observed in convalescent donors with peptides spanning the S protein of the ancestral Wuhan sequence and the corresponding variant S peptides. Geomean S-specific responses ranged from 0.07 to 0.08 for CD4$^+$ T cells and 0.08 to 0.10 for CD8$^+$ T cells. No significant difference was observed between the ancestral and VOC S peptide pools (CD4: B.1.1.7 $p = 0.17$; B.1.351 $p = 0.30$; P.1 $p = 0.21$; CAL.20C $p = 0.06$ and CD8: B.1.1.7 $p = 0.15$; B.1.351 $p = 0.25$; P.1 $p = 0.47$; CAL.20C $p = 0.17$ by Wilcoxon test) (Figures 1A–1C). These values (here and in subsequent graphs) are not corrected for multiple comparisons, as a correction would decrease the statistical power for detecting significant differences; therefore, not performing multiple comparison corrections is the more conservative and stringent test.

To further test for potential differences in the recognition of VOCs by these T cells, we calculated fold change values per individual donor (Figures S2A and S2B). We then performed a non-inferiority test on one sample Wilcoxon signed-rank test compared to the lower bound fold change threshold calculated based on technical repeats (Table S3). No significant differences were observed, demonstrating that the decreases observed were within the range expected from technical repeat variation.

The VOC T cell analyses were extended using FluoroSPOT to measure the capacity of the various SARS-CoV-2 peptide pools to elicit functional responses in terms of secretion of IFN-γ and interleukin-5 (IL-5) cytokines (Figures 1D, 1E, and S2C). The results from the FluoroSPOT assay (Figures 1D and 1E) showed *ex vivo* IFN-γ reactivity using whole PBMCs, with a geomean of 45 SFCs/10^6 PBMCs (range 20–1,578) for the ancestral strain peptides. This overlaps with the 0–800 SFC range (median 110) detected in a previous study describing S reactivity in symptomatic donors[49] and with the 20–110 range for 2–5 months' symptomatic donors reported in a separate study.[50]

VOC reactivity was observed for the S MPs in convalescent donors, with geomean IFN-γ SFCs per million PBMCs ranging from 38 to 45 (Figure 1D). Compared to the ancestral strain, there were significant decreases of 12%, 6%, and 14% for the B.1.1.7, B.1.351, and CAL.20C variant pools (B.1.1.7 $p = 0.02$; B.1.351 $p = 0.03$; P.1 $p = 0.07$, and CAL.20C $p < 0.01$ by Wilcoxon test), while no difference was observed for P.1 (Figure 1D).

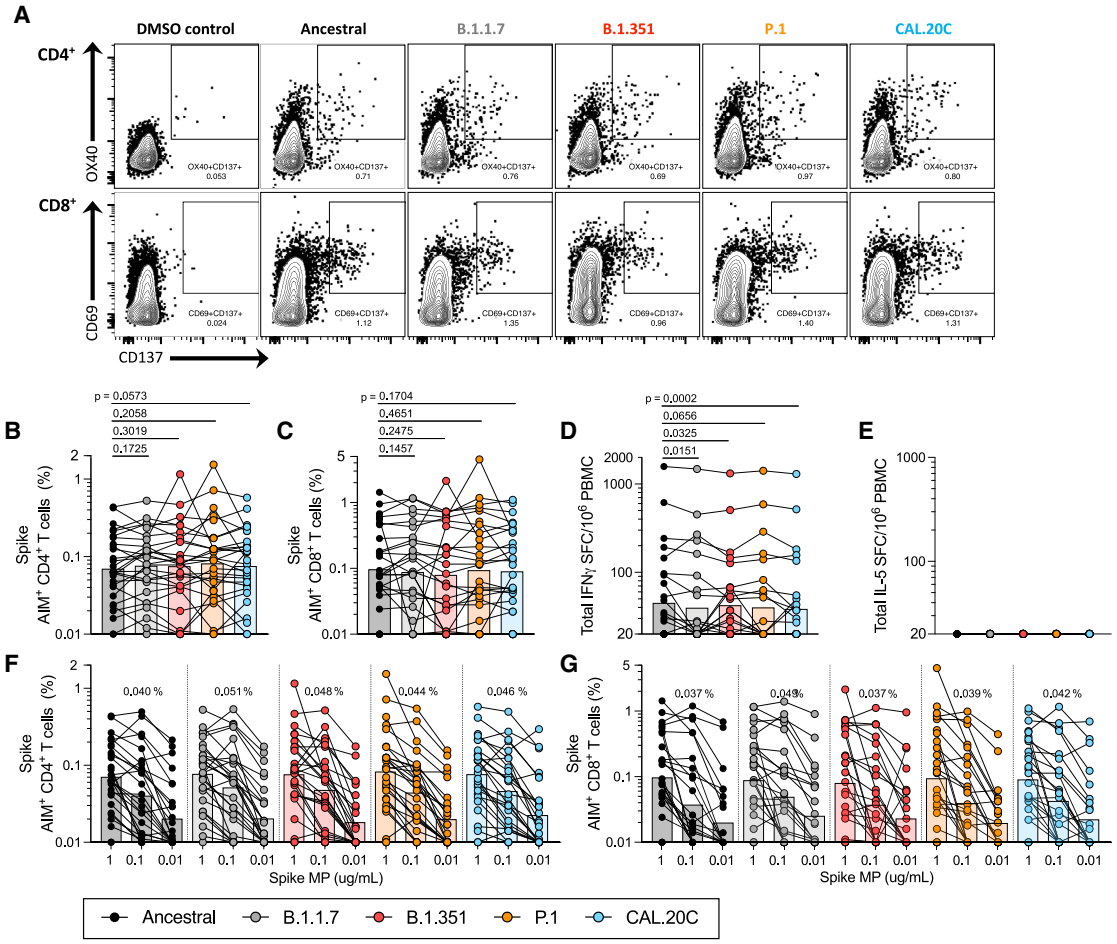

Figure 1. T cell responses of COVID-19 convalescent individuals against ancestral and variant SARS-CoV-2 spike (S)

PBMCs of COVID-19 convalescent individuals (n = 28) were stimulated with the S MPs corresponding to the ancestral reference strain (black) and the B.1.1.7 (gray), B.1.351 (red), P.1 (orange), and CAL.20C (light blue) SARS-CoV-2 variants.

(A) The gating strategy for the AIM assay is illustrated by representative graphs defining S-specific $CD4^+$ or $CD8^+$ T cells by expression of $OX40^+CD137^+$ and $CD69^+CD137^+$, respectively. These graphs depict 1 of the COVID-19 convalescent donors from this study tested with the S MPs corresponding to each of the VOCs tested.

(B) Percentages of AIM^+ ($OX40^+CD137^+$) $CD4^+$ T cells.

(C) Percentages of AIM^+ ($CD69^+CD137^+$) $CD8^+$ T cells.

(D) IFN-γ spot-forming cells (SFCs) per million PBMCs.

(E) IL-5 SFCs per million PBMCs.

(F and G) The data shown in (B) and (C) are plotted to show the titration of the S MPs (1 μg/mL, 0.1 μg/mL, and 0.01 μg/mL) for $CD4^+$ (F) and $CD8^+$ (G) T cells for each SARS-CoV-2 variant. The geometric mean of the 0.1 μg/mL condition is listed above each titration.

Paired comparisons of ancestral S MPs versus each of the variants were performed by 1-tailed Wilcoxon test and are indicated by the p values in (B)–(D). In all of the panels, the bars represent the geometric mean. See also Figures S1, S2, S4, and S5 and Tables S1–S3.

No significant differences were observed by fold change analysis, suggesting that the decreases observed were still within the technical fluctuation range (Figure S2C). No IL-5 reactivity was observed for any of the pools (Figure 1E).

To further assess the functionality of T cell recognition of these variants, we considered the variant peptide dose-response curves of the $CD4^+$ and $CD8^+$ T cells. As shown in Figures 1F and S2D, peptide concentration sensitivity of $CD4^+$ T cell responses to the ancestral and four variant pools was similar. The same pattern was also observed for $CD8^+$ T cell responses to S (Figures 1G and S2E).

$CD4^+$ and $CD8^+$ T cell total reactivity against VOCs

As shown in Table S1, mutations found in the variants studied herein were not limited to the S protein, but also occurred in several additional antigens encoded in the SARS-CoV-2 genome. To address the potential impact of non-S variant mutations on overall proteome-wide $CD4^+$ and $CD8^+$ T cell reactivity, we tested overlapping peptide MPs spanning the entire proteome of the ancestral Wuhan sequence in comparison with corresponding MPs representing the different variants.

Overall, reactivity to the peptide pools spanning the variant genomes was found to be similar to that against the ancestral

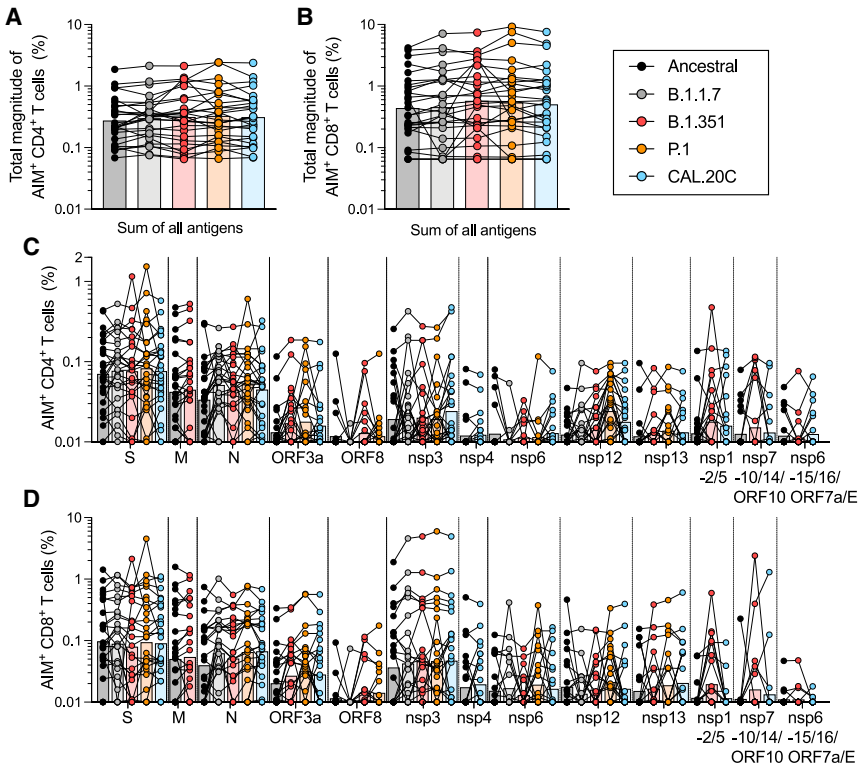

Figure 2. T cell responses of COVID-19 convalescent individuals against ancestral and variant SARS-CoV-2 proteomes

PBMCs of COVID-19 convalescent individuals (n = 28) were stimulated with MPs for the entire viral proteome corresponding to the ancestral reference strain (black) and the B.1.1.7 (gray), B.1.351 (red), P.1 (orange), and CAL.20C (light blue) SARS-CoV-2 variants.

(A) Percentages of AIM$^+$ (OX40$^+$CD137$^+$) CD4$^+$ T cells for the total reactivity.

(B) Percentages of AIM$^+$ (CD69$^+$CD137$^+$) CD8$^+$ T cells for the total reactivity.

(C) Percentages of AIM$^+$ (OX40$^+$CD137$^+$) CD4$^+$ T cells for each MP.

(D) Percentages of AIM$^+$ (CD69$^+$CD137$^+$) CD8$^+$ T cells for each MP.

All of the bars represent the geometric mean. See also Figure S1, S2, S4, and S5 and Tables S1–S3.

CD4$^+$ and CD8$^+$ T cell reactivity against VOCs by vaccinees

We also studied T cell responses by individuals who received US Food and Drug Administration (FDA)-authorized COVID-19 mRNA vaccines. We focused our analysis on T cell reactivity to the S antigen of the ancestral strain, which is the basis of the presently used vaccines.

Wuhan strain (Figures 2 and S2). When the sum total of reactivity throughout the genome was considered, no decreases in reactivity compared to the ancestral were noted for the variant pools (Figures 2A–2C, S2F, and S2G).

We previously showed in COVID-19 convalescent subjects that a set of 10 different antigens (nsp3, nsp4, nsp6, nsp12, nsp13, S, ORF3a, M, ORF8, and N) account for 83% and 81% of the total CD4$^+$ and CD8$^+$ T cell response, respectively.[51] Here, a similar overall pattern of dominant antigens was observed (Figures 2C and 2D). It is worth noting that this specific comparison is for illustration purposes only, as this study is not powered to rule out differences in individual antigens.

For comparison purposes, unexposed donors were also tested in the AIM assay, with MPs encompassing the ancestral and variant strains (Figures S2H–S2M). As expected, some T cell reactivity against the SARS-CoV-2 MPs was observed in unexposed donors, possibly due to previous exposure to common cold coronaviruses[47,48,52,53] or to other pathogens or autoantigens. The magnitude of the responses was lower than in COVID-19 convalescents (unexposed versus convalescent: CD4 $p < 0.0001$; CD8 $p < 0.0001$ by the Mann-Whitney test, comparison not shown in the graphs). Similar to the COVID-19 convalescents, no decrease in the geomean of AIM$^+$ CD4$^+$ or CD8$^+$ T cell responses to the sum of all of the antigens of individual MPs tested was observed in unexposed donors (Figures S2H–S2K). These experiments suggest that CD4$^+$ and CD8$^+$ T cells from individuals infected with the ancestral SARS-CoV-2 strain recognize VOCs with similar efficiency.

For both CD4$^+$ and CD8$^+$ T cell reactivity, the magnitude of responses to pools encompassing the sequences from the ancestral Wuhan genome and the VOCs ranged from a geomean of 0.15–0.17 for CD4$^+$ T cells and a geomean of 0.10–0.15 for CD8$^+$ T cells (Figures 3A–3C). Comparison of the variant pools to the ancestral sequence showed no significant differences for CD4$^+$ and CD8$^+$ T cell reactivity in the AIM assay for B.1.1.7 and P.1 (CD4: B.1.1.7 $p = 0.41$, P.1 $p = 0.29$; CD8: B.1.1.7 $p = 0.10$, P.1 $p = 0.09$ by Wilcoxon test). Decreases of 14% and 22%, respectively, were observed with the B.1.351 pools for CD4$^+$ and CD8$^+$ T cells (B.1.351: $p < 0.01$ for both comparisons), and a 10% decrease with the CAL.20C pool for CD8$^+$ T cells ($p = 0.04$) (Figures 3A–3C). The FluoroSPOT assay (Figures 3D–3F and S3C) showed IFN-γ reactivity, with geomeans ranging from 58 to the 74 SFCs per million PBMCs (Figures 3C and S3C). Given the number of comparisons made and that the reductions observed were on the low side (and others showed increases), we wanted to put these numbers into context by comparing them to what is expected based on the observed fold changes in repeat measurements of the same samples on different days for both AIM and FluoroSPOT assays, and asked whether the observed decreases were significantly higher (non-inferiority analysis; see Method details). No significant differences were observed, indicating that the magnitude of decreases for some strains was within the expected technical assay variability (Figures S3A–S3C). Minimal IL-5 responses were observed, with geomean reactivity ranging from 22 to 23 SFCs/10^6, which is slightly above the limit of detection (Figure 3E). On a per-donor basis, the IFN-γ response was found to account for >80% of the total response,

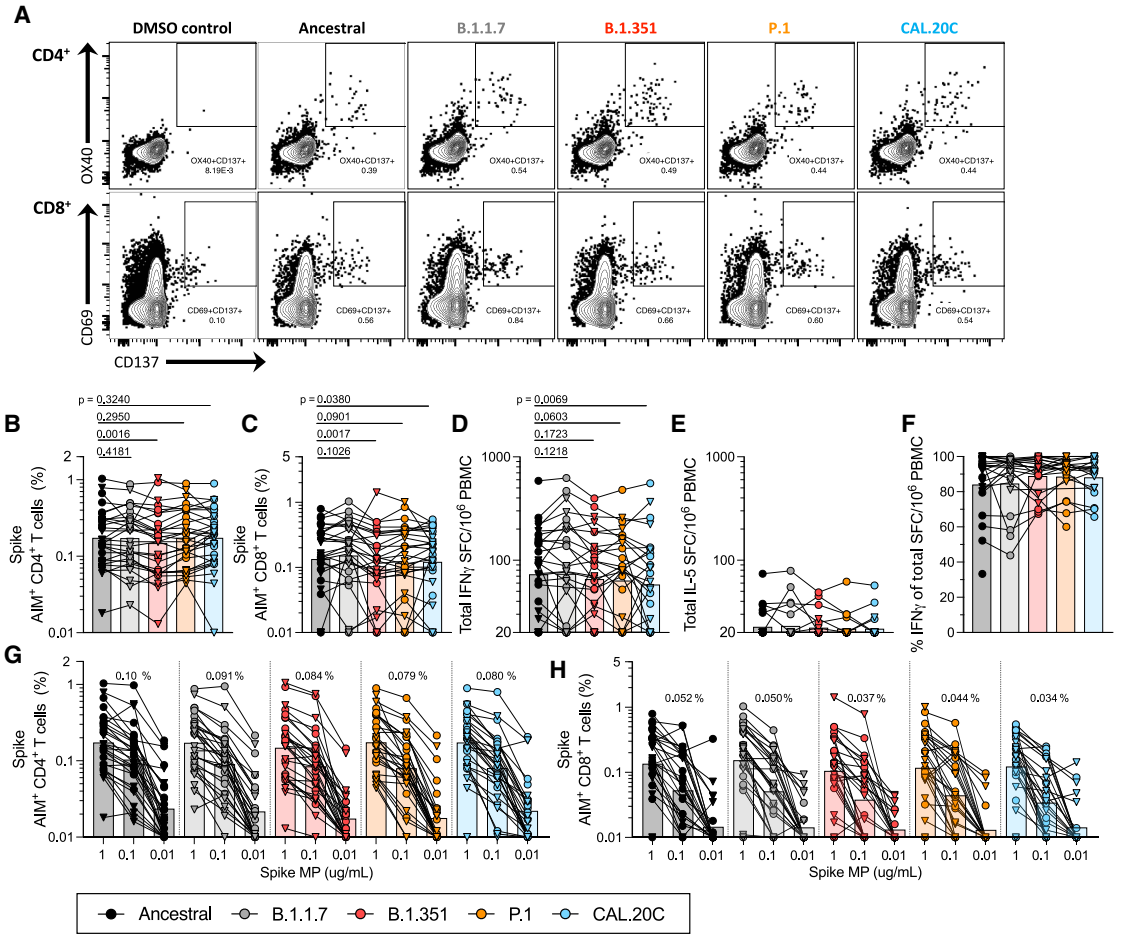

Figure 3. T cell responses of COVID-19 vaccinees against ancestral and variant SARS-CoV-2 S

PBMCs of Pfizer/BioNTech BNT162b2 (n = 14, triangles) and Moderna mRNA-1273 COVID-19 vaccinees (n = 15, circles) were stimulated with the S MPs corresponding to the ancestral reference strain (black) and the B.1.1.7 (gray), B.1.351 (red), P.1 (orange), and CAL.20C (light blue) SARS-CoV-2 variants.

(A) The gating strategy for the AIM assay is illustrated by representative graphs defining S-specific $CD4^+$ or $CD8^+$ T cells by the expression of $OX40^+CD137^+$ and $CD69^+CD137^+$, respectively. These graphs depict one of the COVID-19 vaccinated donors from this study tested with the S MPs corresponding to each of the VOCs tested.

(B) Percentages of AIM^+ ($OX40^+CD137^+$) $CD4^+$ T cells.

(C) Percentages of AIM^+ ($CD69^+CD137^+$) $CD8^+$ T cells.

(D) IFN-γ SFCs per million PBMCs.

(E) IL-5 SFCs per million PBMCs.

(F) Percentages of IFN-γ were calculated from the total IFN-γ and IL-5 SFCs per million PBMCs.

(G and H) The data shown in (B) and (C) are also plotted showing the S MPs titration (1, 0.1, and 0.01 μg/mL) for $CD4^+$ (G) and $CD8^+$ (H) T cells with each SARS-CoV-2 variant. The geometric mean of the 0.1 μg/mL condition is listed above each titration.

Paired comparisons of the ancestral reference strain-based S MP versus each of the variants were performed by one-tailed Wilcoxon test and are indicated by the p values in (B)–(D). In all of the panels, the bars represent the geometric mean. See also Figures S1 and S3–S5 and Tables S1–S3.

on average (range 84%–89%), irrespective of whether the ancestral strain or VOCs were considered (Figure 3F).

Similar to the experiments in convalescent donors, we also examined T cell dose responses in vaccinated donors. As shown in Figures 3G, 3H, S3D, and S3E, $CD4^+$ and $CD8^+$ T cell dose responses to the ancestral and VOC S pools were similar.

Phenotypes of $CD4^+$ and $CD8^+$ T cells

We further assessed the quality of AIM^+ T cell responses by phenotyping S-specific $CD4^+$ and $CD8^+$ AIM^+ T cell responses. Representative gating strategy is shown in Figure S5. Consistent with previous observations,[39,48] AIM^+ T cell responses in COVID-19 convalescent donors above the threshold of positivity (CD4 >0.016% and CD8 >0.16%, as described in Method details; Figure S4), irrespective of the variant analyzed, had a memory phenotype, preferentially enriched for central (Tcm) and effector memory (Tem) phenotypes for $CD4^+$ T cells ($CD4^+$Tcm $CD45RA^+CCR7^-$ and $CD4^+$Tem $CD45RA^-CCR7^-$) (Figure S4A) and Tem phenotypes for $CD8^+$ T cells ($CD8^+$Temra $CD45RA^+CCR7^-$) (Figure S4B). Likewise, AIM^+ T cell responses

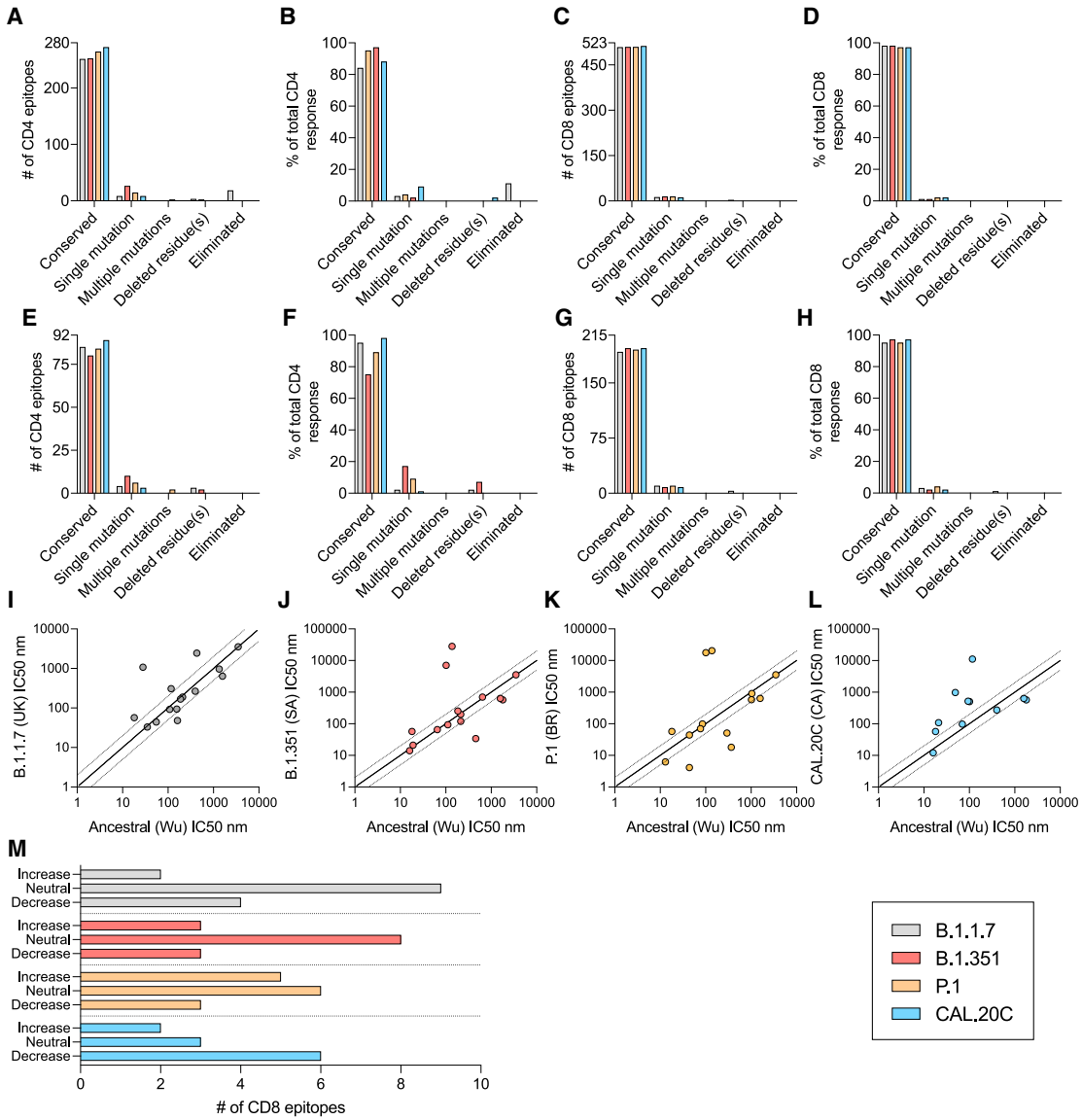

Figure 4. SARS-CoV-2 T cell epitope sequences affected by the variants

CD4$^+$ and CD8$^+$ T cell epitopes of the ancestral strain identified in a previous study[51] were analyzed as a function of the number and percentage of responses that are or are not conserved across the B.1.1.7 (gray), B.1.351 (red), P.1 (orange), and CAL.20C (light blue) SARS-CoV-2 variants.

(A–D) The SARS-CoV-2 epitopes for the most immunodominant SARS-CoV-2 proteins in terms of numbers and percentage of response are shown for CD4$^+$ (A and B) and CD8$^+$ (C and D) T cells.

(E–H) The SARS-CoV-2 epitopes for the S protein only in terms of numbers and percentage of response are shown for CD4$^+$ (E and F) and CD8$^+$ (G and H) T cells.

(I–M) The peptide-binding algorithm data of mutated versus wild-type epitopes are shown for CD8$^+$ (I–L) and for the effect of the mutations on CD8$^+$ T cell epitopes, in which each instance was categorized as a function of whether the binding capability of the mutated peptide was increased (>2-fold), neutral, or decreased (<2-fold) (M).

See also Table S4.

in COVID-19 vaccinees had a memory phenotype regardless of the origin of the SARS-CoV-2 sequences analyzed, with preferential enrichment for Tcm and Tem for CD4 (Figure S4C) and Tem and Temra for CD8 (Figure S4D). This provides additional evidence that donors primed by the ancestral strain S protein, by either infection or vaccination, mount a memory T cell response able to cross-recognize the SARS-CoV-2 VOCs.

Conservation analysis of sets of defined CD4$^+$ and CD8$^+$ T cell epitopes

An analysis of experimentally defined CD4 and CD8 epitopes is presented in Figure 4 and examines both the number of epitopes and the experimentally determined magnitude of responses associated with the epitopes. Specifically, we recently reported a comprehensive study of epitopes recognized in convalescent

subjects, leading to the identification of 280 different $CD4^+$ T cell epitopes.[51] Here, we analyzed how many of those epitopes would be affected by mutations in the different variants. As shown in Figure 4A, we found that 89.6%, 90%, 94.3%, and 97.1% (average 93%) of the $CD4^+$ T cell epitopes are conserved in the B.1.1.7, B1.351, P.1, and CAL.20C variants. A similar pattern is observed when the magnitude of T cell responses associated with the various epitopes is considered, rather than the simple number of epitopes. Fully conserved $CD4^+$ T cell epitopes can be inferred to account for 84.4%, 88.1%, 95.7%, and 97.8% (average 91.5%) of the recognition of the B.1.1.7, B.1.351, P.1, and CAL.20C variants, respectively, based on the ancestral sequence (Figure 4B).

That same study also reported 523 $CD8^+$ T cell epitopes.[51] Performing a similar analysis, 508 (97.1%) of these 523 $CD8^+$ T cell epitopes are totally conserved within the B.1.1.7 variant, 509 (97.3%) within the B.1.351 and P.1 variants, and 512 (97.9%) within the CAL.20C variant (Figure 4C). Similarly, in terms of magnitude of the $CD8^+$ T cell responses associated with the various epitopes, fully conserved $CD8^+$ T cell epitopes can be inferred to account for 98.3%, 98.4%, 97.9%, and 97.8% of the recognition of the B.1.1.7, B.1.351, P.1, and CAL.20C variants, respectively, based on the ancestral sequence (Figure 4D, average of 98.1%).

Finally, we analyzed the degree of $CD4^+$ and $CD8^+$ T cell epitope conservation with an analysis restricted to epitopes in the S antigen. The number of S-derived epitopes conserved at 100% sequence identity was, on average, 84.5% for the $CD4^+$ T cell epitopes (Figure 4E) and 95.3% for the $CD8^+$ T cell epitopes (Figure 4G). Similarly, in terms of magnitude of $CD4^+$ T cell responses to S epitopes, fully conserved $CD4^+$ T cell epitopes can be inferred to account for 95.5%, 75.3%, 89.8%, and 98.3% of the recognition of B.1.1.7, B.1.351, P.1, and CAL.20C variants, respectively, with an average of 89.7% (Figure 4F). For $CD8^+$ T cell responses, fully conserved epitopes can be inferred to account for 95.2%, 97.6%, 95.4%, and 97.3% of the recognition of B.1.1.7, B.1.351, P.1, and CAL.20C variants, respectively, with an average of 96.4% (Figure 4H).

While human leukocyte antigen (HLA) restriction of the class II epitopes[51] could not be unequivocally assigned, the restriction of the class I epitopes was implicitly inferred based on HLA allele-specific predictions and testing in HLA-matched donors. Accordingly, we analyzed the predicted binding affinity for each epitope and matching variant for the corresponding putative HLA class I restriction element. The predicted binding affinity for each ancestral epitope/matching variant for B.1.1.7, B.1.351, P.1, and CAL.20C variants is shown in Figures 4I–4L, tabulated in Table S4, and summarized in Figure 4M. The predicted binding capacity was determined using the NetMHCpan BA 4.1 tool provided by the Immune Epitope Database's (IEDB's) analysis resource.[54,55] In the case of the B.1.1.7, B.1.351, P.1, and CAL.20C variants, the number of mutations associated with binding capacity decreases (conservatively defined as a 2-fold reduction) was 4 out of 15, 3 out of 14, 3 out of 14, and 6 out of 11, respectively.

In conclusion, the analyses suggest that the vast majority of $CD4^+$ and $CD8^+$ T cell epitopes are unaffected by mutations found in all of the different variants. The corresponding mutations are also predicted to have minor effects on the total T cell response, thus providing a molecular basis for the overall impact on T cell reactivity by COVID-19 convalescent subjects and recipients of COVID-19 mRNA vaccines.

DISCUSSION

The present study addresses a key knowledge gap pertaining to the potential of emergent SARS-CoV-2 variants to evade overall recognition by human immune responses. We focused on T cell responses elicited by either natural infection or vaccination with the Pfizer/BioNTech and Moderna COVID-19 mRNA vaccines. We found similar total $CD4^+$ or $CD8^+$ T cell reactivity against the four variants investigated herein, B.1.1.7, B.1.351, P.1, and CAL.20C lineages found initially in the United Kingdom, South Africa, Brazil, and California, respectively. To assess the overall total T cell functionalities, the comparison between the original Wuhan isolate and the variants was performed using different T cell methodologies, such as the AIM assay (quantifying T cells with a range of functionalities), and the FluoroSPOT assay (quantifying cells with specific cytokine-secreting activity). We also tested whether any of the variant sequences may be associated with an altered cytokine polarization.

The data herein provide some positive news in light of justified concern over the impact of SARS-CoV-2 VOCs on the efforts to control and eliminate the present pandemic. Multiples of the VOCs are associated with increased transmissibility, and several have been associated with decreased susceptibility to neutralizing antibodies from infected or vaccinated individuals. In contrast, the data presented here suggest that the total T cell responses are not significantly disrupted by the VOCs. While it is not anticipated that circulating memory T cells would be effective in preventing SARS-CoV-2 infection, it is plausible that they can contribute in reducing COVID-19 severity.[33,56] Several lines of evidence support this notion, such as observations that early SARS-CoV-2 T cell responses are associated with milder COVID-19.[34,35] Thus, the T cell response may contribute to limiting COVID-19 severity induced by VOCs that partially or largely escape neutralizing antibodies. This is consistent with T cell-mediated immunity observed in humans against a different respiratory pathogen, influenza, for which heterologous immunity against diverse influenza strains is associated with memory T cells to conserved epitopes.[57–59]

Our data also provide insights on the predicted impact of the mutations associated with the variants analyzed on T cell responses in the context of the T cell epitopes recognized. Prior reports have identified a large number of T cell epitopes recognized throughout the SARS-CoV-2 proteome, including S.[40,53,60–63] We furthered this point by an analysis of the Tarke et al. dataset, showing that 93% of $CD4^+$ and 97% of $CD8^+$ T cell epitopes in SARS-CoV-2 are completely conserved in the variants. Furthermore, we found that even in the epitopes affected by single mutations, no negative effect on the predicted HLA-binding capacity in the majority of cases is expected. Overall, it is plausible to hypothesize that single amino acid substitutions or deletions across large peptidomes do not significantly affect a polyclonal memory T cell response. Nevertheless, the methodology applied in this study is not powered to reveal whether T cells specific to amino acid sequences that are changed in variant strains still retain functionality. The apparent higher conservation of $CD8^+$ T cell epitopes is to be expected

based on the shorter length of HLA class I binding peptides (usually 9–10 amino acids) as compared to their class II counterparts (13–17 amino acids). This effect is counterbalanced by $CD8^+$ T cells being generally less tolerant of amino substitutions as compared to $CD4^+$ T cells.[47,64] Marginal IL-5 production was detected in all of the conditions tested. This is relevant, since it was reported that single amino acid replacements in an epitope sequence can lead to a change in the cytokines produced,[65,66] and a Th2-like response pattern was initially hypothesized to be linked to adverse outcomes in SARS-specific responses.[67] Overall, we observed that VOC mutations do not significantly disrupt the total $CD4^+$ and $CD8^+$ T cell responses.

VOC mutations could be reflective of adaptation in terms of optimizing replication or binding to ACE2, but also reflective of adaptation to escape immune recognition by antibodies.[13,14,22,68,69] Higher viral binding to a cellular receptor can be a mechanism of compensatory viral evolution in the presence of neutralizing antibodies.[70] In that respect, while mutations to escape antibody binding have been well documented for influenza[71–73] and SARS-CoV-2, immune escape at the level of T cell responses in human populations has not been reported for acute respiratory infections. Because of HLA polymorphism, the epitope repertoire recognized is likely to be substantially different from one individual to the next, greatly decreasing the likelihood of immune escape by an acute virus. An advantage conferred to the virus by a mutation in one person would not be linked to an immune response escape advantage in a non-HLA-matched individual. For SARS-CoV-2, this property of T cell recognition is further enhanced by the fact that the T cell responses against SARS-CoV-2 are highly multiantigenic and multi-specific, with tens of different epitopes recognized by $CD4^+$ and $CD8^+$ T cells in a given individual.[51,52,60,62] Nevertheless, our data do not rule out that certain individuals could be strongly affected by the mutations in specific VOCs.

These results here have potential implications for engineering coronavirus vaccines with broader protective immunity against VOCs. Clearly, the most straightforward path is to update the current vaccines to target a variant S, given how highly successful several COVID-19 vaccines have proven to be against the parental SARS-CoV-2 strain. Our results suggest that a parallel alternative approach could involve the inclusion of additional antigens and T cell epitopes, perhaps selected on the basis of low mutational propensity,[74] to ensure that neutralizing antibodies are complemented with T cell responses to minimize COVID-19 morbidity and mortality.

Limitations of the study

The present study did not assess decreases in antibody reactivity, as several other studies have already investigated this matter.[11,14–20,22,23] Our studies used overlapping peptide pools. As such, we cannot exclude that some of the mutations may involve alterations in terms of antigen processing for either class I or class II, which would be undetected by using pools of "preprocessed" peptides. While we have no reason to suspect that substantial differences may exist between the epitope specificity of responses elicited by different vaccines, our study did not address this point.

The statistical power of this study does not allow for the sensitivity needed to detect the loss of small populations of T cell clones that may be affected by variant sequences when sampled in the presence of the majority of conserved peptides. Alterations in major histocompatibility complex (MHC) binding do not necessarily confer changes in T cell receptor (TCR) affinity, as often several MHC-binding residues can be changed before changing TCR signaling, so we cannot exclude impaired T cell recognition of those specific mutated peptides. An additional limitation of the study in this respect is that one amino acid difference could influence TCR signal strength and memory T cell reactivation. However, each epitope can be recognized by multiple TCRs, and calculating the affinity would require cloning the multiple TCRs recognizing each of the epitopes seen in a polyclonal setting.

Our study was designed to test for differences in total T cell response against the different variants and was not powered or designed to investigate differences between the mRNA vaccines or at the single-peptide level. Furthermore, in our study, the sequences of the infecting virus were not determined, and therefore we cannot exclude that some of the donors may have been exposed to variants. To minimize this issue, the tested samples from convalescent donors were selected to be infected before October 2020; thus, it is unlikely that any of the donors would have been infected by any of the VOCs, as this date precedes their diffusion to an appreciable degree in the United States in general, and California in particular. While we could not clearly define the infecting strain in the COVID-19 convalescent, we showed similar results in vaccinated subjects in whom the response was induced by the ancestral S sequence. As also mentioned in the Results section, the cohorts investigated were predominantly White, reflective of the patient population available for recruitment.

Finally, we have only investigated whether the total T cell responses induced by the ancestral reference sequence are able to cross-recognize variant sequences, as this is relevant to the present situation. We have not examined whether responses induced by an infection with a variant sequence will be able to cross-recognize the ancestral reference sequence present in the approved vaccines.

STAR★METHODS

Detailed methods are provided in the online version of this paper and include the following:

- KEY RESOURCES TABLE
- RESOURCE AVAILABILITY
  - Lead contact
  - Materials availability
  - Data and code availability
- EXPERIMENTAL MODEL AND SUBJECT DETAILS
  - Convalescent COVID-19 donors
  - COVID-19 vaccinees
  - Unexposed donors
- METHOD DETAILS
  - Isolation of peripheral blood mononuclear cells (PBMCs) and plasma
  - SARS-CoV-2 RBD ELISA
  - Mutation analysis of SARS-CoV-2 B.1.1.7, B.1.351, P.1 and CAL.20C variants
  - SARS-CoV-2 Wuhan and variant peptide synthesis and pooling

- Bioinformatic analysis of T cell epitopes
- Flow cytometry-based AIM assay
- FluoroSPOT assay

● QUANTIFICATION AND STATISTICAL ANALYSIS

SUPPLEMENTAL INFORMATION

Supplemental information can be found online at https://doi.org/10.1016/j.xcrm.2021.100355.

ACKNOWLEDGMENTS

This study has been funded by the NIH NIAID (SARS-CoV-2 Assessment of Viral Evolution program, award no. AI142742 to S.C. and A. Sette, contract no. 75N9301900065 to A. Sette and D.W., contract no. 75N93019C00001 to A. Sette and B.P., NIH grant U01 CA260541-01 to D.W., K08 award AI135078 to J.M.D., AI036214 to D.M.S., and HHSN75N93019C00076 to R.H.S.). Additional support has been provided by UCSD T32s (AI007036 and AI007384 to S.A.R. and S.I.R.) and the Jonathan and Mary Tu Foundation (to D.M.S.). A.T. was supported by a PhD student fellowship through the Clinical and Experimental Immunology Course at the University of Genoa, Italy. We thank Gina Levi and the LJI clinical core for assistance in sample coordination and blood processing. We gratefully thank the authors from the originating laboratories responsible for obtaining the specimens, as well as the submitting laboratories where the genome data were generated and shared via GISAID and on which this research is based. We would like to thank Vamseedhar Rayaprolu and Erica Ollmann Saphire for providing the recombinant SARS-CoV-2 RBD protein used in the ELISA assay.

AUTHOR CONTRIBUTIONS

Conceptualization, A.T., A.G., S.C., and A. Sette.; data curation and bioinformatic analysis, Y.Z., R.H.S., and B.P.; formal analysis, A.T., J.S., and A.G.; funding acquisition, S.C., A.S., D.W., S.I.R., S.A.R., and J.M.D.; investigation, A.T., N.M., A. Sutherland, B.G., J.S., E.D.Y., E.W., D.W., A. Sette, and A.G.; project administration, A.F.; resources, S.I.R., S.A.R., and J.M.D.; supervision, J.S., S.C., D.W., A. Sette, R.d.S.A., and A.G.; writing, A.T., D.W., S.C., A. Sette, and A.G.

DECLARATION OF INTERESTS

A. Sette is a consultant for Gritstone, Flow Pharma, CellCarta, Arcturus, Oxford-immunotech, and Avalia. S.C. is a consultant for Avalia. All of the other authors declare no competing interests. LJI has filed for patent protection for various aspects of vaccine design and identification of specific epitopes.

Received: February 27, 2021
Revised: June 7, 2021
Accepted: June 24, 2021
Published: July 2, 2021

REFERENCES

1. Kirby, T. (2021). New variant of SARS-CoV-2 in UK causes surge of COVID-19. Lancet Respir. Med. *9*, e20–e21.
2. Volz, E., Mishra, S., Chand, M., Barrett, J.C., Johnson, R., Geidelberg, L., Hinsley, W.R., Laydon, D.J., Dabrera, G., O'Toole, Á., et al.; COVID-19 Genomics UK (COG-UK) consortium (2021). Assessing transmissibility of SARS-CoV-2 lineage B.1.1.7 in England. Nature *593*, 266–269.
3. Davies, N.G., Abbott, S., Barnard, R.C., Jarvis, C.I., Kucharski, A.J., Munday, J.D., Pearson, C.A.B., Russell, T.W., Tully, D.C., Washburne, A.D., et al.; CMMID COVID-19 Working Group; COVID-19 Genomics UK (COG-UK) Consortium (2021). Estimated transmissibility and impact of SARS-CoV-2 lineage B.1.1.7 in England. Science *372*, eabg3055.
4. Tegally, H., Wilkinson, E., Lessells, R.J., Giandhari, J., Pillay, S., Msomi, N., Mlisana, K., Bhiman, J.N., von Gottberg, A., Walaza, S., et al. (2021). Sixteen novel lineages of SARS-CoV-2 in South Africa. Nat. Med. *27*, 440–446.
5. Voloch, C.M., da Silva Francisco, R., Jr., de Almeida, L.G.P., Cardoso, C.C., Brustolini, O.J., Gerber, A.L., Guimarães, A.P.C., Mariani, D., da Costa, R.M., Ferreira, O.C., Jr., et al.; Covid19-UFRJ Workgroup, LNCC Workgroup, Adriana Cony Cavalcanti (2021). Genomic characterization of a novel SARS-CoV-2 lineage from Rio de Janeiro, Brazil. J. Virol. *95*, e00119-21.
6. Faria, N.R., Mellan, T.A., Whittaker, C., Claro, I.M., Candido, D.D.S., Mishra, S., Crispim, M.A.E., Sales, F.C.S., Hawryluk, I., McCrone, J.T., et al. (2021). Genomics and epidemiology of the P.1 SARS-CoV-2 lineage in Manaus, Brazil. Science *372*, 815–821.
7. Zhang, W., Davis, B.D., Chen, S.S., Sincuir Martinez, J.M., Plummer, J.T., and Vail, E. (2021). Emergence of a Novel SARS-CoV-2 Variant in Southern California. JAMA *325*, 1324–1326.
8. Deng, X., Garcia-Knight, M.A., Khalid, M.M., Servellita, V., Wang, C., Morris, M.K., Sotomayor-González, A., Glasner, D.R., Reyes, K.R., Gliwa, A.S., et al. (2021). Transmission, infectivity, and antibody neutralization of an emerging SARS-CoV-2 variant in California carrying a L452R spike protein mutation. medRxiv, 2021.2003.2007.21252647.
9. Rambaut, A., Loman, N., Pybus, O., Barclay, W., Barrett, J., Carabelli, A., Connor, T., Peacock, T., Robertson, D.L., and Volz, E.; COVID-19 Genomics Consortium UK (CoG-UK (2020). Preliminary genomic characterisation of an emergent SARS-CoV-2 lineage in the UK defined by a novel set of spike mutations. https://virological.org/t/preliminary-genomic-characterisation-of-an-emergent-sars-cov-2-lineage-in-the-uk-defined-by-a-novel-set-of-spike-mutations/563.
10. Washington, N.L., Gangavarapu, K., Zeller, M., Bolze, A., Cirulli, E.T., Barrett, K.M.S., Larsen, B.B., Anderson, C., White, S., Cassens, T., et al. (2021). Genomic epidemiology identifies emergence and rapid transmission of SARS-CoV-2 B.1.1.7 in the United States. medRxiv. https://doi.org/10.1101/2021.2002.2006.21251159.
11. Greaney, A.J., Loes, A.N., Crawford, K.H.D., Starr, T.N., Malone, K.D., Chu, H.Y., and Bloom, J.D. (2021). Comprehensive mapping of mutations in the SARS-CoV-2 receptor-binding domain that affect recognition by polyclonal human plasma antibodies. Cell Host Microbe *29*, 463–476.e6.
12. Starr, T.N., Greaney, A.J., Addetia, A., Hannon, W.W., Choudhary, M.C., Dingens, A.S., Li, J.Z., and Bloom, J.D. (2021). Prospective mapping of viral mutations that escape antibodies used to treat COVID-19. Science *371*, 850–854.
13. Zahradník, J., Marciano, S., Shemesh, M., Zoler, E., Chiaravalli, J., Meyer, B., Dym, O., Elad, N., and Schreiber, G. (2021). SARS-CoV-2 RBD *in vitro* evolution follows contagious mutation spread, yet generates an able infection inhibitor. bioRxiv. https://doi.org/10.1101/2021.2001.2006.425392.
14. Wang, P., Nair, M.S., Liu, L., Iketani, S., Luo, Y., Guo, Y., Wang, M., Yu, J., Zhang, B., Kwong, P.D., et al. (2021). Antibody resistance of SARS-CoV-2 variants B.1.351 and B.1.1.7. Nature *593*, 130–135.
15. Skelly, D.T., Harding, A.C., Gilbert-Jaramillo, J., Knight, M.L., Longet, S., Brown, A., Adele, S., Adland, E., and Brown, H., et al.; Medawar Laboratory Team (2021). Vaccine-induced immunity provides more robust heterotypic immunity than natural infection to emerging SARS-CoV-2 variants of concern. Research Square, 10.21203/rs.3.rs-226857/v2.
16. Wu, K., Werner, A.P., Koch, M., Choi, A., Narayanan, E., Stewart-Jones, G.B.E., Colpitts, T., Bennett, H., Boyoglu-Barnum, S., Shi, W., et al. (2021). Serum Neutralizing Activity Elicited by mRNA-1273 Vaccine. N. Engl. J. Med. *384*, 1468–1470.
17. Muik, A., Wallisch, A.K., Sänger, B., Swanson, K.A., Mühl, J., Chen, W., Cai, H., Maurus, D., Sarkar, R., Türeci, Ö., et al. (2021). Neutralization of SARS-CoV-2 lineage B.1.1.7 pseudovirus by BNT162b2 vaccine-elicited human sera. Science *371*, 1152–1153.
18. Supasa, P., Zhou, D., Dejnirattisai, W., Liu, C., Mentzer, A.J., Ginn, H.M., Zhao, Y., Duyvesteyn, H.M.E., Nutalai, R., Tuekprakhon, A., et al. (2021).

Reduced neutralization of SARS-CoV-2 B.1.1.7 variant by convalescent and vaccine sera. Cell *184*, 2201–2211.e7.

19. Edara, V.V., Norwood, C., Floyd, K., Lai, L., Davis-Gardner, M.E., Hudson, W.H., Mantus, G., Nyhoff, L.E., Adelman, M.W., Fineman, R., et al. (2021). Infection- and vaccine-induced antibody binding and neutralization of the B.1.351 SARS-CoV-2 variant. Cell Host Microbe *29*, 516–521.e3.
20. Shen, X., Tang, H., McDanal, C., Wagh, K., Fischer, W., Theiler, J., Yoon, H., Li, D., Haynes, B.F., Sanders, K.O., et al. (2021). SARS-CoV-2 variant B.1.1.7 is susceptible to neutralizing antibodies elicited by ancestral spike vaccines. Cell Host Microbe *29*, 529–539.e3.
21. Stamatatos, L., Czartoski, J., Wan, Y.H., Homad, L.J., Rubin, V., Glantz, H., Neradilek, M., Seydoux, E., Jennewein, M.F., MacCamy, A.J., et al. (2021). mRNA vaccination boosts cross-variant neutralizing antibodies elicited by SARS-CoV-2 infection. Science *372*, 1413–1418.
22. Wang, Z., Schmidt, F., Weisblum, Y., Muecksch, F., Barnes, C.O., Finkin, S., Schaefer-Babajew, D., Cipolla, M., Gaebler, C., Lieberman, J.A., et al. (2021). mRNA vaccine-elicited antibodies to SARS-CoV-2 and circulating variants. Nature *592*, 616–622.
23. Wibmer, C.K., Ayres, F., Hermanus, T., Madzivhandila, M., Kgagudi, P., Oosthuysen, B., Lambson, B.E., de Oliveira, T., Vermeulen, M., van der Berg, K., et al. (2021). SARS-CoV-2 501Y.V2 escapes neutralization by South African COVID-19 donor plasma. Nat. Med. *27*, 622–625.
24. Emary, K.R.W., Golubchik, T., Aley, P.K., Ariani, C.V., Angus, B., Bibi, S., Blane, B., Bonsall, D., Cicconi, P., Charlton, S., et al.; COVID-19 Genomics UK Consortium; AMPHEUS Project; Oxford COVID-19 Vaccine Trial Group (2021). Efficacy of ChAdOx1 nCoV-19 (AZD1222) vaccine against SARS-CoV-2 variant of concern 202012/01 (B.1.1.7): an exploratory analysis of a randomised controlled trial. Lancet *397*, 1351–1362.
25. Cele, S., Gazy, I., Jackson, L., Hwa, S.H., Tegally, H., Lustig, G., Giandhari, J., Pillay, S., Wilkinson, E., Naidoo, Y., et al.; Network for Genomic Surveillance in South Africa; COMMIT-KZN Team (2021). Escape of SARS-CoV-2 501Y.V2 from neutralization by convalescent plasma. Nature *593*, 142–146.
26. Voysey, M., Clemens, S.A.C., Madhi, S.A., Weckx, L.Y., Folegatti, P.M., Aley, P.K., Angus, B., Baillie, V.L., Barnabas, S.L., Bhorat, Q.E., et al.; Oxford COVID Vaccine Trial Group (2021). Safety and efficacy of the ChAdOx1 nCoV-19 vaccine (AZD1222) against SARS-CoV-2: an interim analysis of four randomised controlled trials in Brazil, South Africa, and the UK. Lancet *397*, 99–111.
27. Hall, V.J., Foulkes, S., Saei, A., Andrews, N., Oguti, B., Charlett, A., Wellington, E., Stowe, J., Gillson, N., Atti, A., et al. (2021). Effectiveness of BNT162b2 mRNA Vaccine Against Infection and COVID-19 Vaccine Coverage in Healthcare Workers in England, Multicentre Prospective Cohort Study (the SIREN Study). Lancet *397*, 1725–1735.
28. Amit, S., Regev-Yochay, G., Afek, A., Kreiss, Y., and Leshem, E. (2021). Early rate reductions of SARS-CoV-2 infection and COVID-19 in BNT162b2 vaccine recipients. Lancet *397*, 875–877.
29. Dagan, N., Barda, N., Kepten, E., Miron, O., Perchik, S., Katz, M.A., Hernán, M.A., Lipsitch, M., Reis, B., and Balicer, R.D. (2021). BNT162b2 mRNA Covid-19 Vaccine in a Nationwide Mass Vaccination Setting. N. Engl. J. Med. *384*, 1412–1423.
30. Novavax Inc (2021). Novavax COVID-19 Vaccine Demonstrates 89.3% Efficacy in UK Phase 3 Trial. https://ir.novavax.com/2021-01-28-Novavax-COVID-19-Vaccine-Demonstrates-89-3-Efficacy-in-UK-Phase-3-Trial.
31. US Food and Drug Administration (2021). Vaccines and Related Biological Products Advisory Committee February 26, 2021. Sponsor Briefing Document Addendum. https://www.fda.gov/media/146218/download.
32. US Food and Drug Administration (2021). Vaccines and Related Biological Products Advisory Committee February 26, 2021 FDA Briefing Document—Addendum–Sponsor. https://www.fda.gov/media/146218/download.
33. Sette, A., and Crotty, S. (2021). Adaptive immunity to SARS-CoV-2 and COVID-19. Cell *184*, 861–880.
34. Rydyznski Moderbacher, C., Ramirez, S.I., Dan, J.M., Grifoni, A., Hastie, K.M., Weiskopf, D., Belanger, S., Abbott, R.K., Kim, C., Choi, J., et al. (2020). Antigen-Specific Adaptive Immunity to SARS-CoV-2 in Acute COVID-19 and Associations with Age and Disease Severity. Cell *183*, 996–1012.e19.
35. Tan, A.T., Linster, M., Tan, C.W., Le Bert, N., Chia, W.N., Kunasegaran, K., Zhuang, Y., Tham, C.Y.L., Chia, A., Smith, G.J.D., et al. (2021). Early induction of functional SARS-CoV-2-specific T cells associates with rapid viral clearance and mild disease in COVID-19 patients. Cell Rep. *34*, 108728.
36. Muñoz-Fontela, C., Dowling, W.E., Funnell, S.G.P., Gsell, P.S., Riveros-Balta, A.X., Albrecht, R.A., Andersen, H., Baric, R.S., Carroll, M.W., Cavaleri, M., et al. (2020). Animal models for COVID-19. Nature *586*, 509–515.
37. Soresina, A., Moratto, D., Chiarini, M., Paolillo, C., Baresi, G., Foca, E., Bezzi, M., Baronio, B., Giacomelli, M., and Badolato, R. (2020). Two X-linked agammaglobulinemia patients develop pneumonia as COVID-19 manifestation but recover. Pediatr. Allergy Immunol. *31*, 565–569.
38. Baker, D., Roberts, C.A.K., Pryce, G., Kang, A.S., Marta, M., Reyes, S., Schmierer, K., Giovannoni, G., and Amor, S. (2020). COVID-19 vaccine-readiness for anti-CD20-depleting therapy in autoimmune diseases. Clin. Exp. Immunol. *202*, 149–161.
39. Dan, J.M., Mateus, J., Kato, Y., Hastie, K.M., Yu, E.D., Faliti, C.E., Grifoni, A., Ramirez, S.I., Haupt, S., Frazier, A., et al. (2021). Immunological memory to SARS-CoV-2 assessed for up to 8 months after infection. Science *371*, eabf4063.
40. Peng, Y., Mentzer, A.J., Liu, G., Yao, X., Yin, Z., Dong, D., Dejnirattisai, W., Rostron, T., Supasa, P., Liu, C., et al.; Oxford Immunology Network Covid-19 Response T cell Consortium; ISARIC4C Investigators (2020). Broad and strong memory $CD4^+$ and $CD8^+$ T cells induced by SARS-CoV-2 in UK convalescent individuals following COVID-19. Nat. Immunol. *21*, 1336–1345.
41. Breton, G., Mendoza, P., Hägglöf, T., Oliveira, T.Y., Schaefer-Babajew, D., Gaebler, C., Turroja, M., Hurley, A., Caskey, M., and Nussenzweig, M.C. (2021). Persistent cellular immunity to SARS-CoV-2 infection. J. Exp. Med. *218*, e20202515.
42. Dowd, S.M., Zalta, A.K., Burgess, H.J., Adkins, E.C., Valdespino-Hayden, Z., and Pollack, M.H. (2020). Double-blind randomized controlled study of the efficacy, safety and tolerability of eszopiclone *vs* placebo for the treatment of patients with post-traumatic stress disorder and insomnia. World J. Psychiatry *10*, 21–28.
43. Sadoff, J., Le Gars, M., Shukarev, G., Heerwegh, D., Truyers, C., de Groot, A.M., Stoop, J., Tete, S., Van Damme, W., Leroux-Roels, I., et al. (2021). Interim Results of a Phase 1-2a Trial of Ad26.COV2.S Covid-19 Vaccine. N. Engl. J. Med. *384*, 1824–1835.
44. Baden, L.R., El Sahly, H.M., Essink, B., Kotloff, K., Frey, S., Novak, R., Diemert, D., Spector, S.A., Rouphael, N., Creech, C.B., et al.; COVE Study Group (2021). Efficacy and Safety of the mRNA-1273 SARS-CoV-2 Vaccine. N. Engl. J. Med. *384*, 403–416.
45. Keech, C., Albert, G., Cho, I., Robertson, A., Reed, P., Neal, S., Plested, J.S., Zhu, M., Cloney-Clark, S., Zhou, H., et al. (2020). Phase 1-2 Trial of a SARS-CoV-2 Recombinant Spike Protein Nanoparticle Vaccine. N. Engl. J. Med. *383*, 2320–2332.
46. Redd, A.D., Nardin, A., Kared, H., Bloch, E.M., Pekosz, A., Laeyendecker, O., Abel, B., Fehlings, M., Quinn, T.C., and Tobian, A.A.R. (2021). CD8+ T cell responses in COVID-19 convalescent individuals target conserved epitopes from multiple prominent SARS-CoV-2 circulating variants. medRxiv. https://doi.org/10.1101/2021.02.11.21251585.
47. Grifoni, A., Weiskopf, D., Ramirez, S.I., Mateus, J., Dan, J.M., Moderbacher, C.R., Rawlings, S.A., Sutherland, A., Premkumar, L., Jadi, R.S., et al. (2020). Targets of T Cell Responses to SARS-CoV-2 Coronavirus in Humans with COVID-19 Disease and Unexposed Individuals. Cell *181*, 1489–1501.e15.
48. Mateus, J., Grifoni, A., Tarke, A., Sidney, J., Ramirez, S.I., Dan, J.M., Burger, Z.C., Rawlings, S.A., Smith, D.M., Phillips, E., et al. (2020). Selective and cross-reactive SARS-CoV-2 T cell epitopes in unexposed humans. Science *370*, 89–94.

49. Zuo, J., Dowell, A.C., Pearce, H., Verma, K., Long, H.M., Begum, J., Aiano, F., Amin-Chowdhury, Z., Hoschler, K., Brooks, T., et al. (2021). Robust SARS-CoV-2-specific T cell immunity is maintained at 6 months following primary infection. Nat. Immunol. *22*, 620–626.

50. Le Bert, N., Clapham, H.E., Tan, A.T., Chia, W.N., Tham, C.Y.L., Lim, J.M., Kunasegaran, K., Tan, L.W.L., Dutertre, C.A., Shankar, N., et al. (2021). Highly functional virus-specific cellular immune response in asymptomatic SARS-CoV-2 infection. J. Exp. Med. *218*, e20202617. https://doi.org/10.1084/jem.20202617.

51. Tarke, A., Sidney, J., Kidd, C.K., Dan, J.M., Ramirez, S.I., Yu, E.D., Mateus, J., da Silva Antunes, R., Moore, E., Rubiro, P., et al. (2021). Comprehensive analysis of T cell immunodominance and immunoprevalence of SARS-CoV-2 epitopes in COVID-19 cases. Cell Rep. Med. *2*, 100204.

52. Braun, J., Loyal, L., Frentsch, M., Wendisch, D., Georg, P., Kurth, F., Hippenstiel, S., Dingeldey, M., Kruse, B., Fauchere, F., et al. (2020). SARS-CoV-2-reactive T cells in healthy donors and patients with COVID-19. Nature *587*, 270–274.

53. Le Bert, N., Tan, A.T., Kunasegaran, K., Tham, C.Y.L., Hafezi, M., Chia, A., Chng, M.H.Y., Lin, M., Tan, N., Linster, M., et al. (2020). SARS-CoV-2-specific T cell immunity in cases of COVID-19 and SARS, and uninfected controls. Nature *584*, 457–462.

54. Dhanda, S.K., Mahajan, S., Paul, S., Yan, Z., Kim, H., Jespersen, M.C., Jurtz, V., Andreatta, M., Greenbaum, J.A., Marcatili, P., et al. (2019). IEDB-AR: immune epitope database-analysis resource in 2019. Nucleic Acids Res. *47* (*W1*), W502–W506.

55. Reynisson, B., Alvarez, B., Paul, S., Peters, B., and Nielsen, M. (2020). NetMHCpan-4.1 and NetMHCIIpan-4.0: improved predictions of MHC antigen presentation by concurrent motif deconvolution and integration of MS MHC eluted ligand data. Nucleic Acids Res. *48* (*W1*), W449–W454.

56. Lipsitch, M., Grad, Y.H., Sette, A., and Crotty, S. (2020). Cross-reactive memory T cells and herd immunity to SARS-CoV-2. Nat. Rev. Immunol. *20*, 709–713.

57. Greenbaum, J.A., Kotturi, M.F., Kim, Y., Oseroff, C., Vaughan, K., Salimi, N., Vita, R., Ponomarenko, J., Scheuermann, R.H., Sette, A., and Peters, B. (2009). Pre-existing immunity against swine-origin H1N1 influenza viruses in the general human population. Proc. Natl. Acad. Sci. USA *106*, 20365–20370.

58. Sridhar, S., Begom, S., Bermingham, A., Hoschler, K., Adamson, W., Carman, W., Bean, T., Barclay, W., Deeks, J.J., and Lalvani, A. (2013). Cellular immune correlates of protection against symptomatic pandemic influenza. Nat. Med. *19*, 1305–1312.

59. Wilkinson, T.M., Li, C.K., Chui, C.S., Huang, A.K., Perkins, M., Liebner, J.C., Lambkin-Williams, R., Gilbert, A., Oxford, J., Nicholas, B., et al. (2012). Preexisting influenza-specific CD4+ T cells correlate with disease protection against influenza challenge in humans. Nat. Med. *18*, 274–280.

60. Ferretti, A.P., Kula, T., Wang, Y., Nguyen, D.M.V., Weinheimer, A., Dunlap, G.S., Xu, Q., Nabilsi, N., Perullo, C.R., Cristofaro, A.W., et al. (2020). Unbiased Screens Show $CD8^+$ T Cells of COVID-19 Patients Recognize Shared Epitopes in SARS-CoV-2 that Largely Reside outside the Spike Protein. Immunity *53*, 1095–1107.e3.

61. Snyder, T.M., Gittelman, R.M., Klinger, M., May, D.H., Osborne, E.J., Taniguchi, R., Zahid, H.J., Kaplan, I.M., Dines, J.N., Noakes, M.N., et al. (2020). Magnitude and Dynamics of the T-Cell Response to SARS-CoV-2 Infection at Both Individual and Population Levels. medRxiv. https://doi.org/10.1101/2020.07.31.20165647.

62. Nelde, A., Bilich, T., Heitmann, J.S., Maringer, Y., Salih, H.R., Roerden, M., Lübke, M., Bauer, J., Rieth, J., Wacker, M., et al. (2021). SARS-CoV-2-derived peptides define heterologous and COVID-19-induced T cell recognition. Nat. Immunol. *22*, 74–85.

63. Keller, M.D., Harris, K.M., Jensen-Wachspress, M.A., Kankate, V.V., Lang, H., Lazarski, C.A., Durkee-Shock, J., Lee, P.H., Chaudhry, K., Webber, K., et al. (2020). SARS-CoV-2-specific T cells are rapidly expanded for therapeutic use and target conserved regions of the membrane protein. Blood *136*, 2905–2917.

64. Weiskopf, D., Angelo, M.A., Sidney, J., Peters, B., Shresta, S., and Sette, A. (2014). Immunodominance changes as a function of the infecting dengue virus serotype and primary versus secondary infection. J. Virol. *88*, 11383–11394.

65. Evavold, B.D., and Allen, P.M. (1991). Separation of IL-4 production from Th cell proliferation by an altered T cell receptor ligand. Science *252*, 1308–1310.

66. Sloan-Lancaster, J., and Allen, P.M. (1996). Altered peptide ligand-induced partial T cell activation: molecular mechanisms and role in T cell biology. Annu. Rev. Immunol. *14*, 1–27.

67. Peeples, L. (2020). News Feature: avoiding pitfalls in the pursuit of a COVID-19 vaccine. Proc. Natl. Acad. Sci. USA *117*, 8218–8221.

68. Starr, T.N., Greaney, A.J., Hilton, S.K., Ellis, D., Crawford, K.H.D., Dingens, A.S., Navarro, M.J., Bowen, J.E., Tortorici, M.A., Walls, A.C., et al. (2020). Deep Mutational Scanning of SARS-CoV-2 Receptor Binding Domain Reveals Constraints on Folding and ACE2 Binding. Cell *182*, 1295–1310.e20.

69. Andreano, E., Piccini, G., Licastro, D., Casalino, L., Johnson, N.V., Paciello, I., Monego, S.D., Pantano, E., Manganaro, N., Manenti, A., et al. (2020). SARS-CoV-2 escape < em > in vitro < /em > from a highly neutralizing COVID-19 convalescent plasma. bioRxiv. https://doi.org/10.1101/2020.12.28.424451.

70. Hensley, S.E., Das, S.R., Bailey, A.L., Schmidt, L.M., Hickman, H.D., Jayaraman, A., Viswanathan, K., Raman, R., Sasisekharan, R., Bennink, J.R., and Yewdell, J.W. (2009). Hemagglutinin receptor binding avidity drives influenza A virus antigenic drift. Science *326*, 734–736.

71. Doud, M.B., Lee, J.M., and Bloom, J.D. (2018). How single mutations affect viral escape from broad and narrow antibodies to H1 influenza hemagglutinin. Nat. Commun. *9*, 1386.

72. Andrews, S.F., Huang, Y., Kaur, K., Popova, L.I., Ho, I.Y., Pauli, N.T., Henry Dunand, C.J., Taylor, W.M., Lim, S., Huang, M., et al. (2015). Immune history profoundly affects broadly protective B cell responses to influenza. Sci. Transl. Med. *7*, 316ra192.

73. Krammer, F., García-Sastre, A., and Palese, P. (2018). Is It Possible to Develop a "Universal" Influenza Virus Vaccine? Potential Target Antigens and Critical Aspects for a Universal Influenza Vaccine. Cold Spring Harb. Perspect. Biol. *10*, a028845.

74. Gaiha, G.D., Rossin, E.J., Urbach, J., Landeros, C., Collins, D.R., Nwonu, C., Muzhingi, I., Anahtar, M.N., Waring, O.M., Piechocka-Trocha, A., et al. (2019). Structural topology defines protective $CD8^+$ T cell epitopes in the HIV proteome. Science *364*, 480–484.

75. Stadlbauer, D., Amanat, F., Chromikova, V., Jiang, K., Strohmeier, S., Arunkumar, G.A., et al. (2020). SARS-CoV-2 Seroconversion in Humans: A Detailed Protocol for a Serological Assay, Antigen Production, and Test Setup. Curr Protoc Microbiol *57*, e100.

76. Vita, R., Mahajan, S., Overton, J.A., Dhanda, S.K., Martini, S., Cantrell, J.R., Wheeler, D.K., Sette, A., and Peters, B. (2019). The Immune Epitope Database (IEDB): 2018 update. Nucleic Acids Res. *47* (*D1*), D339–D343.

77. Jurtz, V., Paul, S., Andreatta, M., Marcatili, P., Peters, B., and Nielsen, M. (2017). NetMHCpan-4.0: Improved Peptide-MHC Class I Interaction Predictions Integrating Eluted Ligand and Peptide Binding Affinity Data. J Immunol *199* (*9*), 3360–3368.

78. Pickett, B.E., Sadat, E.L., Zhang, Y., Noronha, J.M., Squires, R.B., Hunt, V., Liu, M., Kumar, S., Zaremba, S., Gu, Z., et al. (2012). ViPR: an open bioinformatics database and analysis resource for virology research. Nucleic Acids Res. *40*, D593–D598.

79. Reiss, S., Baxter, A.E., Cirelli, K.M., Dan, J.M., Morou, A., Daigneault, A., Brassard, N., Silvestri, G., Routy, J.P., Havenar-Daughton, C., et al. (2017). Comparative analysis of activation induced marker (AIM) assays for sensitive identification of antigen-specific CD4 T cells. PLoS ONE *12*, e0186998.

80. da Silva Antunes, R., Pallikkuth, S., Williams, E., Esther, D.Y., Mateus, J., Quiambao, L., Wang, E., Rawlings, S.A., Stadlbauer, D., Jiang, K., et al. (2021). Differential T cell reactivity to endemic coronaviruses and SARS-CoV-2 in community and health care workers. J. Infect. Dis., jiab176.

STAR★METHODS

KEY RESOURCES TABLE

REAGENT or RESOURCE	SOURCE	IDENTIFIER
Antibodies		
M5E2 (V500) [anti-CD14]	BD Biosciences	561391 (RRID:AB_10611856)
HIB19 (V500) [anti-CD19]	BD Biosciences	561121 (RRID:AB_10562391)
RPA-T4 (BV605) [anti-CD4]	BD Biosciences	562989 (RRID:AB_2737935)
RPA-T8 (BV650) [anti-CD8]	BioLegend	301042 (RRID:AB_2563505)
RPA-T8 (BUV496) [anti-CD8]	BD Biosciences	612942 (RRID:AB_2870223)
FN50 (PE) [anti-CD69]	BD Biosciences	555531 (RRID:AB_2737680)
Ber-ACT35 (PE-Cy7) [anti-OX40]	Biolegend	350012 (RRID:AB_10901161)
4B4-1 (APC) [anti-CD137]	BioLegend	309810 (RRID:AB_830672)
OKT3 (AF700) [anti-CD3]	Biolegend	317340 (RRID:AB_2563408)
UCHT1 (BUV805) [anti-CD3]	BD Biosciences	612895 (RRID:AB_2870183)
HI100 (BV421) [anti-CD45RA]	Biolegend	304130 (RRID:AB_10965547)
G043H7 (FITC) [anti-CCR7]	Biolegend	353216 (RRID:AB_10916386)
Biological samples		
Convalescent donor blood samples	UC San Diego Health	https://health.ucsd.edu/Pages/default.aspx
Convalescent donor blood samples	La Jolla Institute	https://www.lji.org
Convalescent donor blood samples	BioIVT	https://bioivt.com
COVID-19 vaccinee donor blood samples	La Jolla Institute	https://www.lji.org
Unexposed donor blood samples	San Diego Blood Bank	https://www.sandiegobloodbank.org
Unexposed donor blood samples	La Jolla Institute	https://www.lji.org
Unexposed donor blood samples	Carter Blood Care	https://www.carterbloodcare.org
Chemicals, peptides, and recombinant proteins		
Synthetic peptides	TC Peptide Lab	https://tcpeptidelab.com
SARS-CoV-2 Receptor Binding Domain (RBD) protein	Stadlbauer et al.[75]	N/A
Deposited data		
Ancestral	https://www.ncbi.nlm.nih.gov	NC_045512.2
B.1.1.7	https://www.GISAID.org	EPI_ISL_601443
B.1.351	https://www.GISAID.org	EPI_ISL_660629
B.1.351	https://www.GISAID.org	EPI_ISL_736930
B.1.351	https://www.GISAID.org	EPI_ISL_736932
B.1.351	https://www.GISAID.org	EPI_ISL_736944
B.1.351	https://www.GISAID.org	EPI_ISL_736971
B.1.351	https://www.GISAID.org	EPI_ISL_736966
B.1.351	https://www.GISAID.org	EPI_ISL_736973
B.1.351	https://www.GISAID.org	EPI_ISL_825104
B.1.351	https://www.GISAID.org	EPI_ISL_825120
B.1.351	https://www.GISAID.org	EPI_ISL_825131
P.1	https://www.GISAID.org	EPI_ISL_804823
CAL.20C	https://www.GISAID.org	EPI_ISL_847619
CAL.20C	https://www.GISAID.org	EPI_ISL_847621
CAL.20C	https://www.GISAID.org	EPI_ISL_847643

(*Continued on next page*)

Continued

REAGENT or RESOURCE	SOURCE	IDENTIFIER
Software and algorithms		
IEDB	Vita et al.[76]	https://www.iedb.org
IEDB-AR (analysis resource)	Reynisson et al.[55]	http://tools.iedb.org/main
NetMHCpan BA 4.1	Jurtz et al.[77]	http://tools.iedb.org/mhci/
VIGOR4	Pickett et al.[78]	https://www.viprbrc.org//brc/home.spg?decorator=vipr
FlowJo 10	FlowJo, LLC	https://www.flowjo.com
GraphPad Prism 8.4	GraphPad	https://www.graphpad.com

RESOURCE AVAILABILITY

Lead contact

Further information and requests for resources and reagents should be directed to and will be fulfilled by the Lead Contact, Dr. Alessandro Sette (alex@lji.org).

Materials availability

Aliquots of synthesized sets of peptides utilized in this study will be made available upon request. There are restrictions to the availability of the peptide reagents due to cost and limited quantity.

Data and code availability

The published article includes all data generated or analyzed during this study, and summarized in the accompanying tables, figures and supplemental materials.

EXPERIMENTAL MODEL AND SUBJECT DETAILS

Convalescent COVID-19 donors

Convalescent donors were enrolled at either a UC San Diego Health clinic under the approved IRB protocols of the University of California, San Diego (UCSD; 200236X), or at the La Jolla Institute (LJI; VD-214). All donors were California residents and samples were collected from May to October 2020, before any of the SARS-CoV-2 variants described herein had been detected in California. These donors were referred to the study by a health care provider or were self-referred. The CRO BioIVT provided additional cohorts of COVID-19 convalescent donors who had been confirmed positive for COVID-19 by PCR following the resolution of symptoms. The total cohort of convalescent donors represented both genders (43% male, 57% female) and ranged from 20 to 67 years of age (median 38 years). All samples were either PCR positive or seropositive against SARS-CoV-2 by ELISA, as described below. Details of this convalescent COVID-19 cohort are listed in Table 1. All convalescent COVID-19 donors provided informed consent to participate in the present and future studies at the time of enrollment.

COVID-19 vaccinees

The La Jolla Institute recruited 29 healthy adults who had received the first and second dose of the Pfizer/BioNTech BNT162b2 (n = 14) or Moderna mRNA-1273 COVID-19 vaccines (n = 15). Blood draws took place under IRB approved protocols (LJI; VD-214) two to four weeks after the second dose of the vaccine was administered. All donors had their SARS-CoV-2 antibody titers measured by ELISA, as described below. The cohort of vaccinees ranged from 23 to 67 years of age (median 47 years) and represented both genders (31% male, 69% female). At the time of enrollment in the study, all donors gave informed consent.

Unexposed donors

PBMCs from 23 healthy unexposed donors were used as controls. Healthy donors were recruited by the La Jolla Institute under IRB approved protocols (LJI; VD-214) or Carter Blood Care, where according to the blood center's criteria for eligibility the donors were also eligible for our study. All healthy donors were collected from May 2014 to March 2018 (n = 13). Additional healthy donors were recruited from March to May 2020 by the San Diego Blood Bank (SDBB (n = 10) and were confirmed seronegative for SARS-CoV-2 by ELISA. This cohort was 35% male, 56% female, and 9% unknown and ranged from 21 to 82 years of age (median 34). All donors gave informed consent and permission for their samples to be used for future studies.

METHOD DETAILS

Isolation of peripheral blood mononuclear cells (PBMCs) and plasma

Collection and processing of blood samples was performed as previously described.[39,51] Briefly, whole blood was collected in heparin coated blood bags or in ACD tubes and centrifuged for 15 minutes at 1850 rpm to separate the cellular fraction from the plasma. The plasma was then removed and stored at −20°C. The cellular fraction next underwent density-gradient sedimentation using Ficoll-Paque (Lymphoprep, Nycomed Pharma, Oslo, Norway) to separate the PBMCs as previously described.[64] Isolated PBMCs were cryopreserved in cell recovery media containing 10% DMSO (GIBCO), supplemented with 90% heat inactivated fetal bovine serum (FBS; Hyclone Laboratories, Logan UT) and stored in liquid nitrogen until used in the assays.

SARS-CoV-2 RBD ELISA

Serology to SARS-CoV-2 was determined for all donor cohorts as previously described.[34] Briefly, 96-well half-area plates (ThermoFisher 3690) were coated with 1 ug/mL SARS-CoV-2 Spike (S) Receptor Binding Domain (RBD) and incubated at 4°C overnight. The next day, plates were blocked at room temperature for 2 hours with 3% milk in phosphate buffered saline (PBS) containing 0.05% Tween-20. Heat-inactivated plasma was added to the plates for an additional 90-minute incubation at room temperature followed by incubation with the conjugated secondary antibody, detection, and subsequent data analysis by reading the plates on Spectramax Plate Reader at 450 nm using the SoftMax Pro. The limit of detection (LOD) was defined as 1:3. Limit of sensitivity (LOS) for SARS-CoV-2 infected individuals was established based on uninfected subjects, using plasma from normal healthy donors not exposed to SARS-CoV-2.

Mutation analysis of SARS-CoV-2 B.1.1.7, B.1.351, P.1 and CAL.20C variants

Genome sequences for the variant viruses were downloaded from GISAID. These sequences were screened to select those without ambiguous residues and generated from Illumina sequencing technologies using an in-house sequence QC script. The selected genomic sequences were then translated into protein amino acid sequences using the VIGOR4 tool available on the Virus Pathogen Resource (ViPR).[78] Sequence variations in the variant viruses were derived by comparison with Wuhan-1 (NC_045512.2). One or more representative sequences were considered for the B.1.1.7 (EPI_ISL_601443), B.1.351 (EPI_ISL_660629; EPI_ISL_736930; EPI_ISL_736932; EPI_ISL_736944; EPI_ISL_736966; EPI_ISL_736971; EPI_ISL_736973; EPI_ISL_825104; EPI_ISL_825120; EPI_ISL_825131), P.1 (EPI_ISL_804823), and CAL.20C (EPI_ISL_847619; EPI_ISL_847621; EPI_ISL_847643) variants. A summary of all the amino acids mutated in the different variants considered in this study with respect to the Wuhan sequence and is available in Table S1.

SARS-CoV-2 Wuhan and variant peptide synthesis and pooling

Peptides were synthesized that spanned entire SARS-CoV-2 proteins and corresponded to the ancestral Wuhan sequence or the B.1.1.7, B.1.351, P.1 and CAL.20C SARS-CoV-2 variants. Peptides were 15-mers overlapping by 10 amino acids and were synthesized as crude material (TC Peptide Lab, San Diego, CA). All peptides were individually resuspended in dimethyl sulfoxide (DMSO) at a concentration of 10–20 mg/mL. Megapools (MP) for each antigen were created by pooling aliquots of these individual peptides, undergoing another lyophilization, and resuspending in DMSO at 1 mg/mL.

Bioinformatic analysis of T cell epitopes

The binding capacity of SARS-CoV-2 T cell epitopes, and their corresponding variant-derived peptides, for their putative HLA class I restricting allele(s) was determined utilizing the NetMHCpan BA 4.1 algorithm,[55] as implemented by the IEDB's analysis resource.[54,76] Predicted binding is expressed in terms of IC_{50} nM. For each epitope-variant pair a ratio of affinities (variant IC_{50} nM/WT IC_{50} nM) was determined. Ratios > 2, indicating a 2-fold or greater decrease in affinity due to the mutation, were accordingly categorized as a decrease in binding capacity, and a ratio < 0.5 as an increase; ratios between 0.5 and 2 were designated as neutral.

Flow cytometry-based AIM assay

Activation induced cell marker (AIM) assay has previously been described in detail elsewhere.[39,79,80] In summary, PBMCs were cultured in the presence of SARS-CoV-2-specific (ancestral or VOC) MPs [1 μg/ml] in 96-well U-bottom plates at a concentration of $1x10^6$ PBMC per well. As a negative control, an equimolar amount of DMSO was used to stimulate the cells in triplicate wells and as positive controls phytohemagglutinin (PHA, Roche, 1 μg/ml) and a cytomegalovirus MP (CMV, combining CD4 and CD8 MPs, 1 μg/ml) were also included. After incubation for 20–24 hours at 37°C, 5% CO_2, the cells were stained with CD3 BUV805 or CD3 AF700 (4:100 or 4:100; BD Biosciences Cat# 612895 or Life Technologies Cat# 56-0038-42, respectively), CD4 BV605 (4:100; BD Biosciences Cat# 562658), CD8 BUV496 or BV650 (2:100 or 4:100; BD Biosciences Cat# 612942 or Biolegend Cat# 301042), CD14 V500 (2:100; BD Biosciences Cat# 561391), CD19 V500 (2:100; BD Biosciences Cat# 561121), and Live/Dead eFluor506 (5:1000; eBioscience Cat# 65-0866-14). Cells were also stained to measure activation with the following markers: CD137 APC (4:100; Biolegend Cat# 309810), OX40 PE-Cy7 (2:100; Biolegend Cat#350012), and CD69 PE (10:100; BD Biosciences Cat# 555531). The memory phenotyping was analyzed by staining with CD45RA (1:100; Biolegend Cat# 304130) and CCR7 (2:100; Biolegend Cat# 353216). All samples were acquired on a ZE5 5-laser or 4-laser cell analyzer (Bio-rad laboratories) and analyzed with

FlowJo software (Tree Star). In the resulting data generated from the AIM assays, the background was removed from the data by subtracting the average of the % of AIM^+ cells plated in triplicate wells stimulated with DMSO. The Stimulation Index (SI) was calculated by dividing the % of AIM^+ cells after SARS-CoV-2 stimulation with the average % of AIM^+ cells in the negative DMSO control. An SI greater than 2 and a minimum of 0.016% or 0.16% AIM^+ $CD4^+$ or $CD8^+$ cells, respectively, after background subtraction was considered to be a positive response based on the median twofold standard deviation of all negative controls measured in the study (> 80), as previously reported.[39] The gates for AIM^+ cells were drawn relative to the negative and positive controls for each donor. A representative example of the gating strategy is depicted in Figure S5. Specifically, lymphocytes were gated, followed by single cells determination. T cells were considered to be positive for CD3 and negative for a Dump channel including in the same colors CD14, CD19 and Live/Dead staining. The $CD3^+CD4^+$ and $CD3^+CD8^+$ were further gated based on $OX40^+CD137^+$ and $CD69^+CD137^+$ AIM markers, respectively. Memory phenotype was gated based on the expression of CD45RA and CCR7 markers on the $CD3^+CD4^+$ and $CD3^+CD8^+$ T cells and the AIM^+ T cells.

FluoroSPOT assay

96-well FluoroSpot plates were coated with anti-cytokine antibodies for IFNγ and IL-5 (mAbs 1-D1K and TRFK5, respectively; Mabtech, Stockholm, Sweden) at a concentration of 10 μg/mL. PBMCs were stimulated in triplicate at a density of $200x10^3$ cells/well with S MPs corresponding to each of the SARS-CoV-2 variants analyzed (1 μg/mL), PHA (1 μg/mL), and DMSO (0.1%), as positive and negative controls respectively. After 20 hours of incubation at 37°C, 5% CO_2, cells were discarded and plates were washed before the addition of cytokine antibodies (mAbs 7-B6-1-BAM and 5A10-WASP; Mabtech, Stockholm, Sweden). After a 2-hour incubation, plates were washed again with PBS/0.05% Tween20 and incubated for 1 hour with fluorophore-conjugated antibodies (Anti-BAM-490 and Anti-WASP-640). An AID iSPOT FluoroSpot reader (AIS-diagnostika, Germany) was used to count the fluorescent spots that resulted from cells secreting IFNγ and IL-5. Each peptide MP was considered positive compared to the DMSO negative control based on the following criteria: 20 or more spot forming cells (SFC) per 10^6 PBMC after background subtraction, a stimulation index (S.I.) greater than 2, and a p value < 0.05 by either a Poisson or t test calculated between the triplicates of the MP and the relative negative control.

QUANTIFICATION AND STATISTICAL ANALYSIS

Data and statistical analyses were performed in FlowJo 10 and GraphPad Prism 8.4, unless otherwise stated. Statistical details of the experiments are provided in the respective figure legends and in each methods section pertaining to the specific technique applied. Data plotted in logarithmic scales are expressed as geometric mean. Statistical analyses were performed using Wilcoxon matched-pairs signed rank test for paired comparisons. Multi-hypothesis testing corrections (MHTC) have not been applied in the study by design. The study is not designed or powered to address differences across different proteins. The primary hypothesis is that no significant differences are observed across the different variants, and this is more stringently addressed avoiding to correct for MHTC, since a difference that is not significant would remain so even after corrections. Therefore, reporting the data without applying MHTC is a more stringent criterion which is appropriately being applied in this case to avoid false negatives. Details pertaining to significance are also noted in the respective figure legends.

To determine the expected variability of the AIM assays, we also analyzed 23 donors for which $CD4^+$ and $CD8^+$ T cell responses to Spike, M and N megapools were evaluated in up to 4 repeat measurements. A total of 208 measurements were made for these donors for both CD4 and CD8, resulting in 69 independent assessments of repeat measures (comparing the initial measurement to a repeat in the same donor) (Table S3). We evaluated the variability in these repeat measures using a corrected log2 fold-change calculated as:

$$\text{Log2}\ \frac{(\text{measure 1} + \text{LOD})}{(\text{measure 2} + \text{LOD})}$$

where LOD is the level of detection threshold, which is 0.014% for CD4 and 0.06% for CD8 based on the twofold geometric 95%CI of all negative controls measured (> 80). The addition of the LOD ensures that variations between measurements close to- or below the level of detection do not result in inflated fold-change estimates. We evaluated the standard deviation of these corrected log-fold change values of repeat measurements (at an individual level), and used this value as a threshold for what would constitute a significant, non-random change at the population level. Similarly, FluoroSPOT assay variability was evaluated by analyzing 38 donors and a total of 301 measurements considering an LOD of 20 SFC/10^6 cells. For CD4-AIM assays, that corresponded to a corrected fold-change of 2.3, for CD8-AIM of 2.4 and for FluoroSPOT of 1.6 as shown in Table S3. Next, we performed a test of non-inferiority for the observed AIM assay or FluoroSPOT reactivities for any of the variants tested compared to the ancestral strain. A non-inferiority test determines if the observed values are significantly above what would be considered a biological meaningful reduction in responses, based on one sample Wilcoxon Signed Rank test compared to the lower bound fold change threshold. The test results in a p value expressing effectiveness of the comparison and a p value corresponding to the discrepancy. Confidence intervals for discrepancy are shown in all the graphs where the comparison was considered statistically significant ($p < 0.05$). The non-inferiority test found that all CD4 and CD8 responses or IFNγ responses to any of the variant peptide pools were significantly above the lower bound threshold. Therefore, by this approach at the population level, there is no biological meaningful reduction in the T cell response to the variant pools compared to the ancestral strain. Details pertaining to significance are also noted in the respective figure legends.